THE FUNCTIONAL SIGNIFICANCE OF G PROTEIN-COUPLED RECEPTOR DIMERIZATION

by

Matthew R. Whorton

A dissertation submitted in partial fulfillment
of the requirements for the degree of
Doctor of Philosophy
(Pharmacology)
in The University of Michigan
2008

Doctoral Committee:

Assistant Professor Roger K. Sunahara, Chair
Assistant Professor Jorge A. Iñiguez-Lluhí
Professor Jennifer J. Linderman
Professor Richard R. Neubig
Professor William B. Pratt
Associate Professor John J. G. Tesmer

To my parents and Jen for their love, support, and encouragement.

ACKNOWLEDGEMENTS

I would like to thank my advisor Roger Sunahara for his guidance and support. I would also like to extend my gratitude to other members of the Sunahara lab, both past and present, as well as members of the Neubig and Tesmer labs for thoughtful discussions and comments during lab meetings.

I would also like to extend a great deal of gratitude to several collaborators who have provided their expertise to various aspects of my research. At Stanford University, Mike Bokoch and Soren Rasmussen in Brian Kobilka's lab and Bo Huang in Richard Zare's lab were instrumental in fluorescently labeling β_2AR and then imaging it with their powerful TIRF single molecule setup. Beata Jastrzebska and Paul Park in Krzysztof Palczewski's lab at Case Western University were also invaluable in providing purified rhodopsin as well as performing transducin activation assays. And finally, I would like to thank Dimitrios Fotiadis in Andrea Engel's lab for using their various microscopy techniques to image rhodopsin-HDL complexes.

I would also like to thank my friends and roommates through out the years who have helped to enrich the graduate school experience. I am also indebted to my fiancée Jen and my family for their love and support.

TABLE OF CONTENTS

LIST OF FIGURES

Figure

LIST OF ABBREVIATIONS

AC	Adenylyl Cyclase
AFM	Atomic Force Microscopy
apoAI	Apolipoprotein A-I
β_2AR	β_2 Adrenergic Receptor
Bis(NHS)PEO_5	*bis N*-succinimidyl[pentaethylene glycol] ester
B_{max}	Maximum Receptor Binding
BRET	Bioluminescence Resonance Energy Transfer
BS^3	Bis(sulfosuccinimidyl) Suberate
cAMP	Cyclic Adenosine Monophosphate
CFP	Cyan Fluorescent Protein
cGMP	Cyclic Guanosine Monophosphate
CHAPS	3-[(3-Cholamidopropyl)dimethylammonio]-1-propanesulfonate
CMC	Critical Micelle Concentration
CNG	Cyclic Nucleotide Gated Channel
Con A	Concanavalin A
CREB	cAMP Response Element Binding Protein
DDM	Dodecyl Maltoside
DHAP	Dihydroalprenolol
DOPC	Dioleoyl Phosphocholine
EDTA	Ethylenediaminetetraacetic Acid
EM	Electron Microscopy
ERK	Extracellular Signal-Regulated Kinase

FRET	Fluorescence Resonance Energy Transfer
G protein	GTP-binding protein
GABA	Gamma-aminobutyric Acid
GDP	Guanosine Diphosphate
GIRK	G Protein-Coupled Inwardly-Rectifying Potassium Channel
GPCR	G Protein-Coupled Receptor
GRK	G Protein-Coupled Receptor Kinase
GTP	Guanosine Triphosphate
GTPγS	Guanosine 5'-O-(3-thiotriphosphate)
HDL	High Density Lipoprotein
HEK	Human Embryonic Kidney
IP	Immunoprecipitate
ISO	Isoproterenol
K_{high}	High Affinity K_i
K_i	Inhibitory Constant
K_{low}	Low Affinity K_i
LtB4	Leukotriene B4
MAP	Mitogen-Activated Protein
META	Metarhodopsin
mGluR	Metabotropic Glutamate Receptor
MLCK	Myosin Light Chain Kinase
MWCO	Molecular Weight Cutoff
PBS	Phosphate Buffered Saline
PDE	Phosphodiesterase
PI	Protease inhibitors
PKA	Protein Kinase A
PLC	Phospholipase C

POPC	Palmitoyl-oleoyl Phosphocholine
POPG	Palmitoyl-oleoyl Phosphoglycerol
RET	Resonance Energy Transfer
RGS	Regulators of G Protein Signaling
rHDL	Reconstituted HDL
ROS	Rod Outer Segment
RT	Room Temperature
SDS-PAGE	Sodium Dodecyl Sulfate - Polyacrylamide Gel Electrophoresis
SEC	Size Exclusion Chromatography
TBS	Tris Buffered Saline
TEM	Transmission Electron Microscopy
TIRF	Total Internal Reflection Fluorescence
TM	Phase Transition Temperature
Tris	Trishydroxymethylaminomethane
UV	Ultraviolet
UV-VIS	Ultraviolet-Visible
WT	Wild Type
YFP	Yellow Fluorescent Protein

ABSTRACT

THE FUNCTIONAL SIGNIFICANCE OF G PROTEIN-COUPLED RECEPTOR DIMERIZATION

by

Matthew R. Whorton

Chair: Roger K. Sunahara

G protein-coupled receptors (GPCRs) are seven transmembrane domain proteins that transduce a diverse array extracellular signals across the plasma membrane and couple to the heterotrimeric family of G proteins. Like most intrinsic membrane proteins, GPCRs are capable of oligomerization and this has led to speculation that GPCR dimers may be required for receptor function and efficient activation of G proteins. One challenge in understanding the function of oligomers relates to the inability to separate monomeric and oligomeric receptor complexes in membrane environments using traditional biochemical approaches. In this thesis, I use a novel reconstitution technique based on high density lipoproteins (HDL) to circumvent this limitation. HDL particles are 10 nm diameter phospholipid bilayer discs surrounded by a dimer of the amphipathic protein apolipoprotein A-I. I first demonstrate that a prototypical GPCR, the β_2 adrenergic receptor (β_2AR), can be incorporated into the phospholipid bilayer of a reconstituted HDL (rHDL) particle together with the stimulatory heterotrimeric G

protein, Gs. Single-molecule fluorescence imaging and fluorescence resonance energy transfer (FRET) analyses demonstrate that a single β_2AR is incorporated per rHDL particle. The monomeric β_2AR efficiently activates Gs and displays GTPγS-sensitive allosteric ligand-binding properties. I also demonstrate that another prototypical GPCR, rhodopsin, is monomeric and functional when incorporated into rHDL particles. The photoreceptor, rhodopsin, has been shown to exist as arrays of dimers in native tissues and thus provides an ideal system for directly comparing the function of monomers and oligomers. Monomeric rhodopsin•rHDL maintains the appropriate spectral properties with respect to photoactivation and formation of the active form, metarhodopsin II. Additionally, the kinetics of metarhodopsin II decay is similar between oligomeric rhodopsin in native membranes and monomeric rhodopsin in rHDL particles. Furthermore, photoactivation of monomeric rhodopsin•rHDL also results in the rapid activation of transducin, at a rate that is comparable to that found in native rod outer segments and 20-fold faster than rhodopsin in detergent micelles. Together, these data suggest that a monomeric receptor in a lipid bilayer is the minimal functional unit necessary for signaling, and that oligomerization is not an absolute requirement for this process.

CHAPTER 1

INTRODUCTION

G Protein-Coupled Receptor Biology

G protein-coupled receptors (GPCRs) are seven transmembrane-spanning receptors that reside on the surface of cells and are responsible for detecting a variety of substances and then transmitting this information inside the cell. These substances range from endogenous compounds such as adrenaline, dopamine, chemokines, and glutamate to exogenous ligands including morphine and tetrahydrocannabinol, as well as sensory stimuli like odors, tastes, and light. The GPCR superfamily is the third largest member of the human genome, consisting of approximately 1000 genes, and because of their vast and varied roles in regulating the body, it is estimated that they are the targets of 30-50% of all medications [1].

GPCRs relay extracellular information into cells by interacting with intracellular G proteins, through a process known as signal transduction. G proteins are a diverse class of heterotrimeric proteins comprised of three subunits: α, β, and γ. There are at least 20 α, 7 β and 12 γ subtypes in humans. The alpha subunits bind guanine nucleotides and are divided into several families: α_s (stimulates adenylyl cyclase (AC)), $\alpha_{i/o}$ (inhibits AC), α_q (stimulates phospholipase C (PLC)), and $\alpha_{12/13}$ (stimulates guanine nucleotide exchange factors) [2]. There also several specialized alpha subunits: α_t, the alpha subunit

of transducin which is activated by the photoreceptor, rhodopsin, and α_{olf} which interacts with olfactory receptors. The β and γ subunits are obligate dimers and can also interact with downstream effectors, such as phospholipase A or the G protein-coupled inwardly-rectifying potassium channel (GIRK). G proteins are also lipid-modified, via the α and γ subunits, which keeps them associated with the plasma membrane and facilitates their interactions with receptors [3, 4].

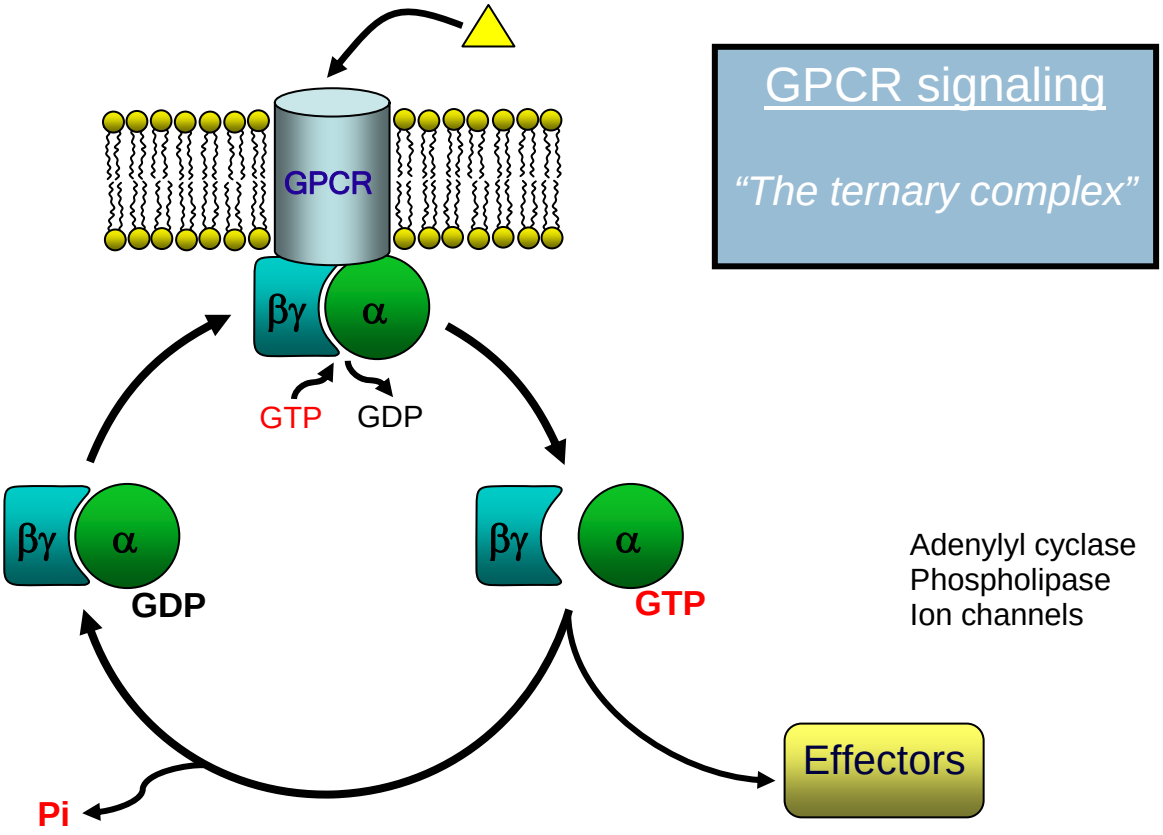

Figure 1-1. The GPCR signaling pathway. Extracellular ligands (yellow triangle) bind to and activate the transmembrane GPCR which then activates a coupled heterotrimeric G protein by stimulating the release of GDP. The subsequent binding of GTP to the α subunit causes the G protein to dissociate into the α and βγ subunits which go on to activate downstream effectors. Hydrolysis of the bound GTP promotes re-association of the two subunits and the cycle can repeat.

In their basal state, G proteins are bound to guanosine diphosphate (GDP). When an agonist binds and activates a receptor, this induces a conformation change in a bound,

or coupled, G protein (***Fig. 1-1***). This conformational change activates the G protein by stimulating the release of GDP and allowing guanosine triphosphate (GTP) to bind, a process driven by the high millimolar concentration of intracellular GTP. An active G protein functionally dissociates into its constituent α and $\beta\gamma$ subunits allowing each subunit to activate downstream effectors. G protein signaling is eventually terminated by the hydrolysis of GTP to GDP. Hydrolysis is achieved through the intrinsic GTPase activity of the α subunit and may be accelerated through an interaction with accessory proteins like RGS (Regulators of G protein Signaling). This drives the re-association of the α and $\beta\gamma$ subunits and the GDP-bound G protein can then rebind a receptor to complete the cycle. Receptors can also be desensitized through the action of G protein-coupled receptor kinases (GRKs). Receptor phosphorylation leads to the binding of arrestin proteins that can block G protein signaling or promote receptor internalization. GRK2 and GRK3, like RGS molecules, contain a conserved 120 amino acid motif that is responsible for binding G protein alpha subunits. Larger roles for RGS molecules, other than GTPase acceleration, have been identified, suggesting that this family of proteins may also be viewed as effectors [5].

The multiple-protein transfer of information, from receptor to G protein to effector, achieves significant signal amplification because activation of one protein at each step may subsequently activate multiple downstream molecules. For instance, in some GPCR systems, a single activated receptor can activate hundreds of G proteins [6], and a single activated $G\alpha_s$ protein can activate adenylyl cyclase and stimulate the synthesis of hundreds of cyclic adenosine monophosphate (cAMP) molecules. cAMP

then activates protein kinase A, which in turn may phosphorylate and modulate the activities of several downstream targets.

Another important aspect of many GPCRs is that they are allosteric proteins. Agonist binding to GPCRs projects an allosteric influence on the G protein to promote nucleotide exchange. In a thermodynamically-coupled fashion, agonist binding is positively cooperative for G protein binding. For instance, the presence of a bound G protein on a receptor can dramatically increase its affinity for a ligand by up to two orders of magnitude [7]. Uncoupling the G protein from the receptor with GTP or non-hydrolyzable GTP analogues disrupts the allosteric effect. This feature, along with the signal amplification discussed above, makes the GPCR signaling pathway remarkably sensitive.

GPCRs are classified into 6 families based on sequence homology and functional similarity: Class A (Rhodopsin-like), Class B (Secretin-like), Class C (Metabotropic glutamate, pheromone and taste receptors), Class D (Fungal pheromone), Class E (cAMP receptors), and the Frizzled/Smoothened class. The Class A family is by far the largest, recognizing a diverse array of ligands, including catecholamines, photons, nucleotides, phospholipids, and peptides. My work has focused on two prototypical Class A receptor systems: rhodopsin and the β_2 adrenergic receptor (β_2AR). These are among the earliest GPCRs to be identified, purified, and cloned and thus have been extensively studied.

Rhodopsin is the receptor in rod cells in the retina that is responsible for scotopic, or low light, vision. It is capable of detecting and responding to a single photon which causes the isomerization of its covalently bound ligand, 11-cis-retinal [8]. The photoisomerization event induces a conformational change in the receptor, similar to

agonist binding in hormone receptors and leads to the activation of the retina-specific G protein, transducin ($G\alpha_t\beta_1\gamma_1$). Activated $G\alpha_t$ binds to and activates the γ-subunit of cyclic guanosine monophosphate (cGMP) phosphodiesterase (PDE6), causing a decrease in cellular cGMP levels. This decreases the probability of cyclic nucleotide gated (CNG) channel opening and promotes hyperpolarization of the cell, a process that is eventually interpreted as a signal [9]. One unique characteristic of rhodopsin is that it is highly organized within the rod cell. It is compartmentalized into special disc-shaped phospholipid sacks near the tip of the cell, called an outer segment. The rod outer segment (ROS) is densely packed, and comprised of over 90 % rhodopsin (***Fig. 1-2***). This highly specialized design gives rod cells the sensitivity to detect single photons.

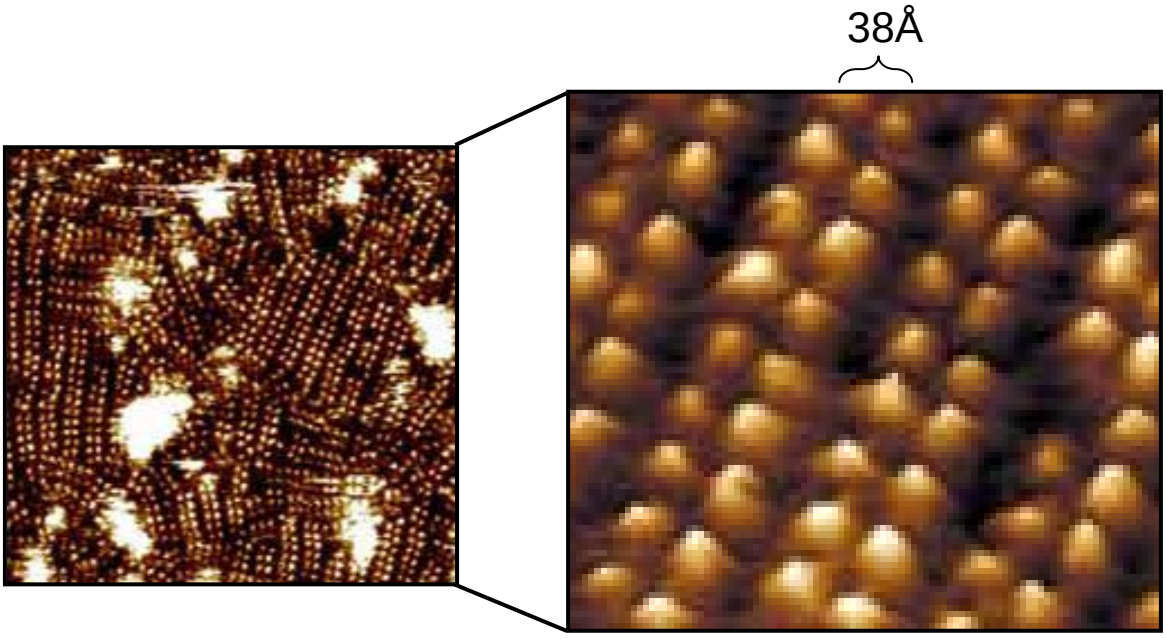

Figure 1-2. Atomic force microscopy of rod outer segment discs from mouse retina. Paracrystalline arrays of rows of dimers of rhodopsin are clearly visible. Within each dimer, the rhodopsin molecules are 38 Å apart, implying that they must be forming physical interactions. Image adapted from Fotiadis *et al.* [10] with permission.

The β_2AR has several roles in the body, including the regulation of smooth muscle relaxation (such as vasodilation and bronchodilation) as well as other processes

such as glycogenolysis and lipolysis. Its physiological importance makes the β_2AR a target for many drugs, including those used in the treatment of asthma and hypertension. The primary signaling pathway for the β_2AR is the activation by endogenous epinephrine, which causes the activation of the stimulatory G protein, G_s. GTP-bound $G\alpha_s$ binds directly to and activates adenylyl cyclase ($G\beta\gamma$ may also regulate adenylyl cyclase but in an isoform-specific manner) causing an increase in cAMP levels and activation of protein kinase A (PKA). PKA mediates various downstream effects. For instance, PKA regulates smooth muscle tone by phosphorylating myosin light chain kinase (MLCK) and impairing its ability to activate myosin. PKA can also regulate the transcription of many genes through activating the transcription factor CREB (cAMP response element binding protein).

In addition, recent work has shown that the β_2AR (as well as other receptors) can signal through a G protein-independent pathway, namely through arrestins [11]. Although arrestin was originally recognized for its involvement in receptor desensitization, this new paradigm gives arrestin a role as a scaffold to activate alternative signaling pathways such as the mitogen-activated protein (MAP) kinase cascade and Src kinase. Hormone activation of GPCRs can therefore regulate both G protein-dependent and G protein-independent pathways. Another interesting and provocative development is the concept of biased agonism and biased signaling. Ligands may serve as an agonist for a G protein pathway but serve as an antagonist for the arrestin pathway, or vice versa [12]. A striking example is ICI-118551, an inverse agonist for the G protein-dependent arm of β_2AR signaling but a potent activator of the MAP kinase pathway [13].

GPCR Oligomerization

Classically, GPCRs have always been considered to act as monomers. That is, the canonical ternary complex where one ligand activates a single receptor which then activates a G protein. However, research as far back as the 1970s has suggested otherwise. For instance, saturation isotherms and competition binding assays yielded data that could not be modeled as a single binding site/receptor, but may be interpreted as a more complex interaction between two receptors within a dimer or oligomer [14, 15]. More direct evidence from target size analysis of the α and β_2 adrenergic receptors [16, 17], as well as cross-linking experiments also suggested that these GPCRs existed as oligomers [18].

Renewed interest in the concept of GPCR dimerization emerged in the 1990s with the advent of complementation experiments initiated by Maggio *et al*. [19]. They demonstrated that co-expression of M3/α2, α2/M3 chimeric receptors could restore binding to the respective receptor types where the individual receptor chimeras lacked binding capacity for any ligand. Other groups have also showed complementation of selectively inactivated mutant receptors. Thus, co-expression of a receptor lacking the ability to bind ligand with one defective in G protein coupling – can restore receptor function [20, 21]. The rationale for these experiments is that the inactive receptor parts are forming functional receptor complexes through dimerization. However, these experiments have been criticized, as the results may only be true for these specific mutants or the result of a recombinant *in cyto* cell system where receptors are highly-overexpressed [22].

It has also been reported that GPCR oligomers may be observed when resolved by SDS polyacrylamide gel electrophoresis (SDS-PAGE). Multiple receptor species were identified by SDS-PAGE with molecular weights consistent with monomers and higher order (dimer and tetramers) arrangements. The proportion of SDS-resistant species could be altered with agonist pre-treatment, or decreased by incubation with a transmembrane-mimetic peptide [23]. GPCR homo- or heterodimers have also been identified by co-immunoprecipitation from cells [24]. However, these techniques have been criticized for their potentially confounding choice of buffer conditions (*e.g.* detergent and salt). For instance, many of the co-IP assays were done by solubilizing the cell membranes with weak non-ionic detergents such as Triton X-100, a detergent known for its capacity to preserve large protein-lipid complexes such as lipid rafts [25]. Caution should be used when referring to the co-IP of a receptor-lipid-receptor complex as a GPCR hetero- or homodimer.

It was not until the development of the biophysical techniques Bioluminescence-, and Fluorescence- Resonance Energy Transfer (BRET and FRET) that the concept of GPCR dimerization started to gain wider acceptance [22, 26, 27]. In the case of FRET either fluorescent donor and acceptor proteins or probes (Cyan Fluorescent Protein, CFP and Yellow Fluorescent Protein, YFP, respectively) are fused to proteins of interest (***Fig. 1-3***). Excitation and the subsequent emission of the donor fluorophore will result in the excitation of a neighboring acceptor fluorophore, provided that it is within in a relatively short distance. This distance, the Förster distance (50-100 Å) is defined as the distance at which the energy transfer between two fluorophores is fifty-percent efficient [28]. This has proved to be a powerful technique for looking at GPCR oligomerization since two

receptors must form a physical interaction in order to be within the Förster distance and yield a significant RET signal.

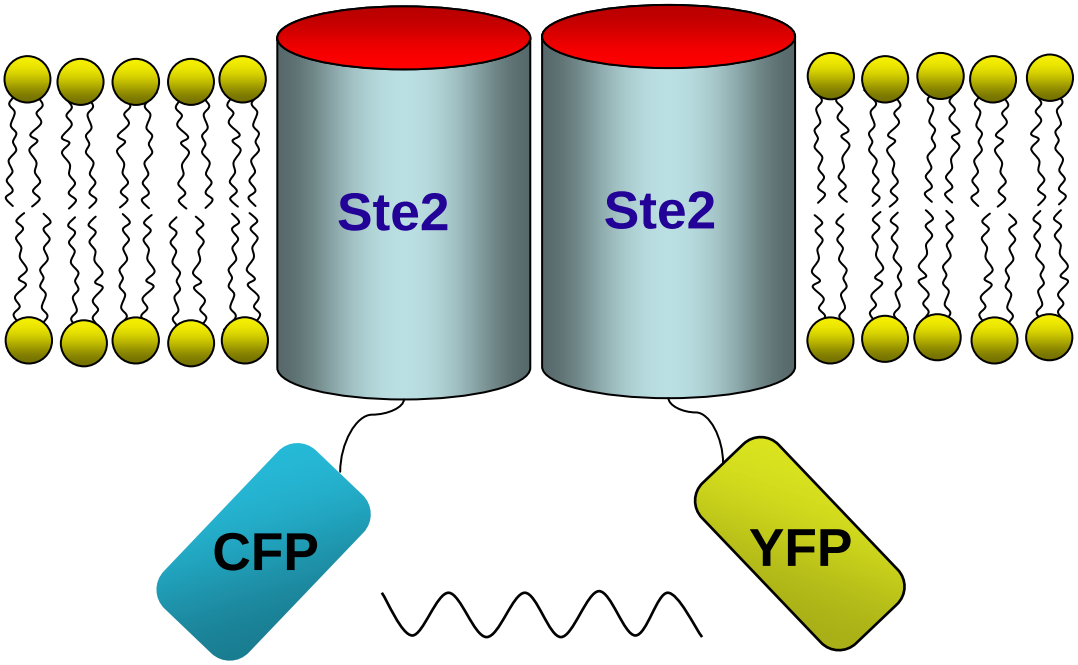

Figure 1-3. Illustration of a typical FRET experimental setup. CFP or YFP are fused to the receptor via the C-terminus. Excitation of CFP will transfer energy to the YFP if the Ste2 receptors are brought close enough through dimerization.

The Bouvier and Blumer groups are credited with first adapting the BRET and FRET techniques towards studying GPCR dimerization. Bouvier's group used BRET to show that the β_2AR existed as homodimers when transiently transfected into HEK 293 cells [27], while the Blumer group used FRET to show that the yeast pheromone receptor, Ste2, was a dimer in *S. cerevisiae* [26]. Since then, BRET and FRET have emerged as the premier techniques for demonstrating that GPCRs can form dimers in cells with over 30 receptors having been shown to dimerize using these methods [22].

Other indirect evidence of GPCR dimerization has also recently emerged. Perhaps the most physiologically relevant example is that of the $GABA_B$ receptor.

Several groups demonstrated that the minimal functional signaling unit of this receptor is a dimer, comprised of $GABA_BR1$ and $GABA_BR2$ protomers [29-31]. The R1 receptor can bind ligand but cannot efficiently traffic to the plasma membrane due to an exposed endoplasmic reticulum retention signal. The R2 subunit, on the other hand, efficiently traffics to the membrane but binds ligands very poorly. Coexpression of the two subunits restores ligand-dependent effector activation in whole cells, implying that the restoration of plasma membrane trafficking and ligand binding was afforded by the heterodimer. A similar scenario has also been demonstrated with the α_{1D} adrenergic receptor. When the α_{1D} receptor is heterologously expressed, it does not traffic to the membrane. However, coexpression with the α_{1B} adrenergic receptor brings a functional α_{1D} to the membrane [32].

Perhaps the most striking evidence of GPCR dimerization comes from imaging studies using Atomic Force Microscopy (AFM) of discs from ROS isolated from mouse retina [10]. In this work, it was observed that rhodopsin exists in ordered arrays of receptor dimers. Furthermore, the close proximity between receptors (38 Å – roughly equal to the diameter of a receptor) implies the formation of meaningful receptor-receptor contacts (***Fig. 1-2***). This provocative finding was highly significant because these observations were made in native tissue and were the first, and to date only, demonstration that GPCR oligomers exist *in vivo*. However, this was also a controversial finding as some have claimed that the results are due to sample preparation artifacts and that the images defy earlier data claiming that rhodopsin is freely diffusible and monomeric in the retina [33].

The overwhelming evidence that GPCRs exist as oligomers begs the question as to their functional relevance. Moreover, many investigators in the field have even suggested that the dimeric receptor must be the minimal functional unit and that a pentameric complex of a receptor dimer and one heterotrimeric G protein is the true signaling unit [34, 35]. It has also been suggested that the allosteric effect of agonists may actually be explained by receptor-receptor cooperativity (which may be modulated by G proteins), rather than by receptor-G protein cooperativity as has generally been assumed [36].

Needless to say, this has recently emerged as a controversial topic and has been the subject of intense research as the consequences of GPCR oligomerization may have significant functional relevance. Because GPCRs are such important drug targets, modulation of the dimer interface and potential receptor-receptor crosstalk represent further avenues for drug development. Also, the concept of receptor heterodimerization introduces a whole new set of druggable targets and would potentially open the door to increasing the specificity of current drugs.

High Density Lipoproteins as a system for studying membrane proteins

The goal of my thesis work was to determine the functional significance of GPCR dimerization. To solve this problem, I took a reductionist approach – that is, to isolate a monomeric receptor in a defined biochemical system and compare its function to receptors in native tissue preparations where it has been previously shown to exist as oligomers. Unfortunately, the major obstacle in this endeavor was the difficulty in

accurately comparing monomeric and oligomeric receptor systems using the current state of the art of membrane protein biochemistry.

The major problem lies in the fact that GPCRs reside in the cell membrane and in order to purify them, they must first be extracted from the membrane. Although detergents are relatively efficient at removing membrane proteins such as GPCRs from cell membranes, they are not adequate substitutes for phospholipids. It has been shown that detergents have deleterious functional effects on a variety of membrane proteins including GPCRs [37-39]. For instance, the detergent dodecyl maltoside impairs the kinetics of photointermediates of rhodopsin and inhibits transducin activation [38].

The traditional route to overcome the deleterious effects of detergent is to reconstitute a purified, detergent-solubilized receptor into phospholipid vesicles. However, this approach presents several drawbacks that were not suitable for our goals. The reconstitution of membrane proteins into phospholipid vesicles is naturally heterogeneous. Typically, a random mixture of vesicles of varying sizes (50-500 nm diameter) is obtained containing between 1 and 1000 receptors [40]. Furthermore, it is exceedingly difficult to control the orientation of the reconstituted receptors, as it has been reported in the literature that receptors can reconstitute in both parallel and anti-parallel fashion [41-43]. Most important is the fact that even if one could reconstitute a small number of receptors into a vesicle, recent work has shown that rhodopsin, in particular, will self-associate into oligomeric complexes [44].

To solve these problems, we adopted a novel reconstitution system originally developed by the Sligar lab that relies on High Density Lipoproteins (HDL). They had adopted this system for studying membrane proteins like P450s [45, 46] and

bacteriorhodopsin [47]. We anticipated that this approach could be used to circumvent the problems we faced in studying GPCR oligomerization.

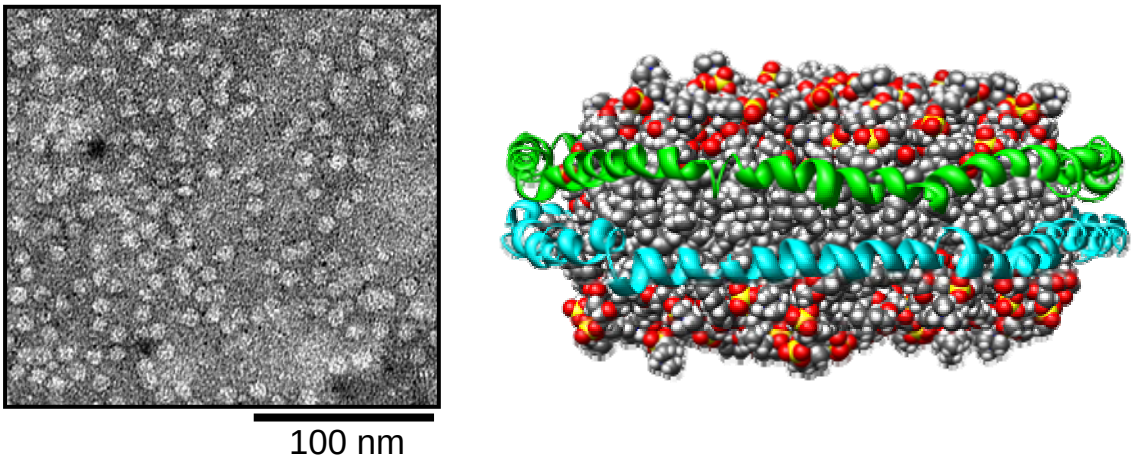

Figure 1-4. High density lipoproteins (HDL). Negative staining electron microscopy shows that HDL is comprised of ~ 10 nm discs (left panel). A molecular model illustrates the quaternary structure of HDL: a phospholipid bilayer wrapped by a dimer of apolipoprotein A-I (cyan and teal) (right panel).

HDL is a protein-lipid complex that is part of the reverse cholesterol transport pathway in the body [48]. It serves to sequester and transport excess cholesterol from the vasculature to the liver for excretion. The most remarkable property about HDL is that nascent HDL is comprised of a 10 nm-diameter phospholipid bilayer that is surrounded and stabilized by a belt made of a dimer of apolipoprotein A-I (apoAI) [49] (***Fig. 1-4***). This bilayer is essentially a cell membrane mimetic and the whole complex can be easily reconstituted *in vitro* by adding defined lipids to purified apoAI, and I refer to these as reconstituted HDL particles (rHDL) [50]. Incorporation of membrane proteins, like GPCRs, into the rHDL phospholipid bilayer is as simple as including purified receptor into the reconstitution mix [47].

The advantages of using the HDL system versus phospholipid vesicles are many and they allow us to address a central question regarding the role of receptor

oligomerization: What is the minimal functional signaling unit required to activate a G protein? The physical properties of HDL particles (their uniformity in size and monodispersion) and their accessibility to G proteins on both sides of the bilayer provide an appropriate system to investigate this question. In this thesis, I will demonstrate that the efficiency of incorporation of GPCRs into HDL is extremely high compared to the relatively poor efficiency observed with phospholipid vesicle reconstitution systems [51]. Due to the relatively small diameter of the HDL particles, there is a theoretical limit on the number of receptors that one may incorporate into the HDL bilayers. As such, I will demonstrate that the incorporated receptors are indeed monomeric [51, 52]. Finally, I will demonstrate that the reconstituted monomeric receptor is fully capable of interacting with and activating a G protein.

CHAPTER 2

A MONOMERIC G PROTEIN COUPLED RECEPTOR EFFICIENTLY COUPLES TO ITS G PROTEIN

Introduction

Oligomerization appears as a common theme for numerous integral membrane proteins. While the role of protein oligomerization is clear for some proteins such as ion channels [53-55] and receptor tyrosine kinases [56], the contribution of oligomerization to G protein-coupled receptor function has become a topic of debate [57-59]. The most compelling case exists for the $GABA_B$ receptor [29-31], where heterodimerization is required for both plasma membrane targeting and G protein activation. Although plasma membrane targeting has been attributed to oligomerization for some Class A GPCRs [60, 61], a more comprehensive functional significance has yet to be discovered. Considering that many GPCRs form physical oligomeric interactions [62-64], including the provocative demonstration that rhodopsin exists as arrays of dimers [57, 65], it seems plausible that GPCRs may function optimally as oligomers. Functional studies on the $GABA_B$ receptor [29-31] as well as biophysical and biochemical evidence from Class A receptors, including rhodopsin [58, 66] and the leukotriene B4 receptor [67], suggest that a pentameric complex, consisting of a GPCR dimer and a G protein heterotrimer, is required for efficient G protein activation.

However, the fundamental question as to whether a monomeric GPCR is capable of coupling efficiently to a G protein in a membrane environment arises from these studies. Efficient coupling should be reflected by receptor-mediated allosteric changes in the G protein structure that result in nucleotide exchange and mutual G protein-dependent effects on receptor affinity for agonists. To address this, we rely on a unique approach for isolating GPCR monomers within high-density lipoproteins (HDL). HDL, comprised of a dimer of apolipoprotein A-I (apoA-I) surrounding a planar bilayer of approximately 160 phospholipids, is easily reconstituted *in vitro* (rHDL) [49, 50]. Electron microscopy of these rHDL particles highlight the disc-shaped structure of approximately 10-12 nm in diameter and thickness of approximately 40 Å, the same thickness of a plasma membrane (***Fig. 2-1a-c***). This reconstitution system has been used by the Sligar laboratory to incorporate various membrane proteins into the phospholipid bilayer, including bacteriorhodopsin [47], cytochrome P450 [68] and the β_2-adrenergic receptor [69]. In this report we utilize the HDL-based reconstitution system to incorporate purified β_2AR and its cognate G protein, Gs. We unambiguously demonstrate that β_2AR reconstituted in HDL (β_2AR•rHDL) is monomeric. We also show that monomeric β_2AR•rHDL is fully functional by virtue of its capacity to support both high-affinity agonist binding and rapid agonist-mediated nucleotide exchange.

Results

Reconstitution of β_2AR into HDL. A variety of conditions were examined for incorporating purified cyan fluorescent protein fused-β_2AR fusion protein (CFP-β_2AR) or wild-type-β_2AR (β_2AR) into HDL disks. By reconstituting CFP-β_2AR into a mixture of

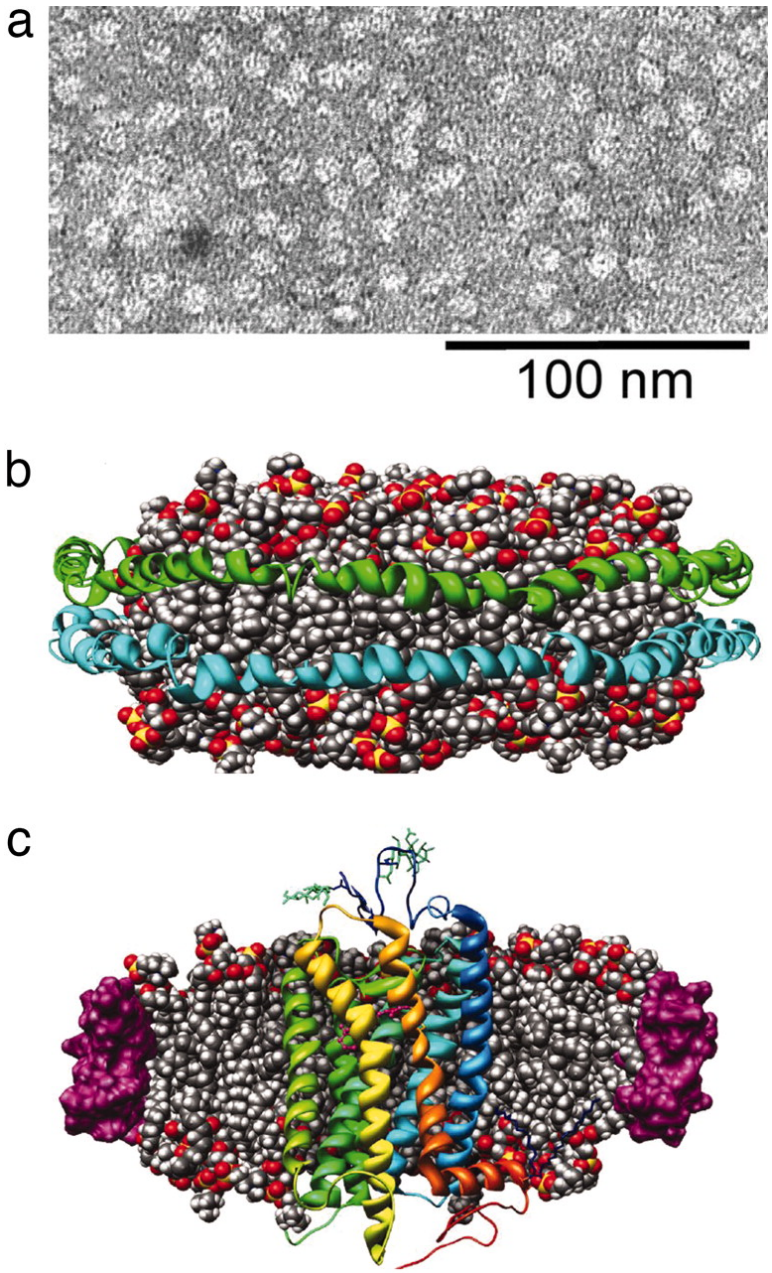

Figure 2-1. Depiction of rHDL particles. **(a)** Transmission electron micrograph of negatively stained rHDL. Well-defined 10-nm rHDL particles are clearly visible. (Scale bar, 100 nm) **(b)** Molecular model illustrating rHDL composed of a dimer of apoA-I proteins wrapped around a phospholipid bilayer composed of 160 POPC molecules (24). Each apoA-I protein (cyan and green) is depicted as a ribbon diagram. **(c)** Molecular model of a GPCR (bovine rhodopsin, Protein Data Bank ID code 1F88) reconstituted into rHDL. Images were generated by using UCSF Chimera Package from the Resource for Biocomputing, Visualization, and Informatics at the University of California, San Francisco (supported by National Institutes of Health Grant P41 RR-01081) (44). Coordinates for the HDL model, from Segrest et al. (24), are used with permission from Stephen Harvey, Georgia Institute of Technology, Atlanta, GA.

lipids (POPC and POPG) and apoA-I we obtained greater than 98% recovery of [^{3}H]DHAP binding activity (***Fig. 2-2a***). CFP-β_2AR•rHDL exhibits binding affinities for antagonists and agonists with K_i values that are more consistent with those observed for β_2AR in biological membranes rather than in detergent micelles as is demonstrated in ***Fig. 2-2b*** and ***Fig. 2-7b,c***. Disks containing β_2AR and fluorophore-labeled receptors (see below) exhibit similar properties (data not shown).

β_2AR in rHDL is monomeric by single molecule spectroscopy. The inner diameter of an HDL particle is estimated to be approximately 85 Å [70]; therefore, we predict that a maximum of two receptors can possibly fit within an rHDL (the receptor diameter is ~ 40 Å, as determined from the rhodopsin crystal structure [71]). Moreover the conditions used for the initial stage of the β_2AR reconstitution (i.e. vast excess of apoA-I:receptor, ratio 100:1, or HDL:receptor of 50:1) favor the incorporation of a single receptor per rHDL.

To make a more definitive assessment of the β_2AR:rHDL stoichiometry, we employed total internal reflection fluorescence (TIRF) microscopy to image single molecules of fluorescently-tagged β_2AR•rHDL (Cy3 or Cy5). The degree of Cy3 and Cy5 label colocalization is related to the fraction of rHDL particles containing two or more receptors, and the fraction of monomeric receptors.

We have determined labeling conditions such that greater than 99 % of β_2ARs are labeled with either Cy3 or Cy5 in detergent micelles (***Fig. 2-3***). In addition, to confirm that the receptor preparations are not oligomeric in detergent micelles prior to labeling and reconstitution, we utilized a crosslinking approach with bifunctional amine-reactive

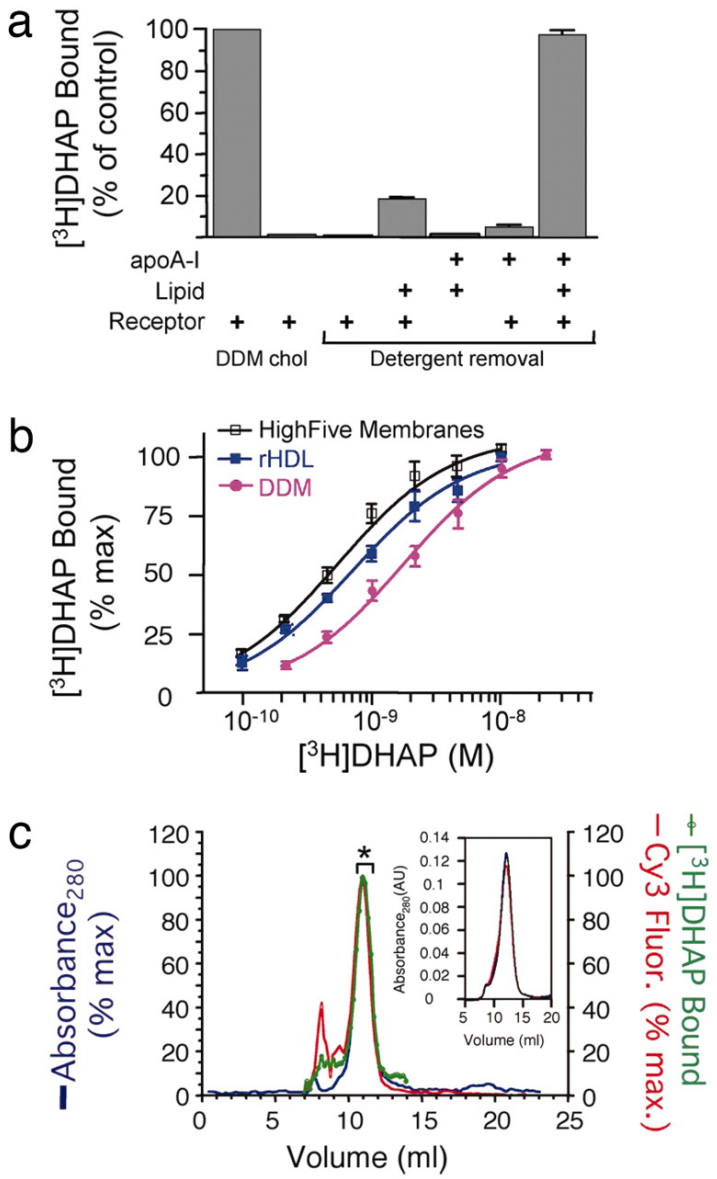

Figure 2-2. Functional reconstitution of beta2AR into rHDL. **(a)** β_2AR requires apoA-I and lipids to survive detergent removal with high efficiency. Equal amounts of DDM-solubilized β_2AR were included in the rHDL reconstitution assay with or without apoA-I and lipid (POPC/palmitoyl-oleoyl-phosphatidylglycerol at 3:2) as described in Materials and Methods and assayed for [^{3}H]DHAP binding (at 20 nM). For comparison, equal amounts of receptor were also assessed for binding activity in the presence of 25 mM cholate ("chol") or 1 % DDM. Data shown are specific binding. **(b)** Saturation-binding assays were performed on β_2AR in HighFive cell membranes (open squares), in DDM micelles (pink filled circles), or in rHDL lipid bilayers (blue filled squares). (c) Cy3-β_2AR·rHDL elutes as a single peak by SEC (Superdex 200; GE Healthcare) as monitored by UV absorbance (blue), [^{3}H]DHAP binding (green), and fluorescence (red). Bracketed area (with asterisk) represents the fractions analyzed for functional and fluorescence studies. (Inset) Preparations of Cy5-β_2AR·rHDL (red) or (Cy3-β_2AR +Cy5-β_2AR)·rHDL (black) elute similarly Cy3-β_2AR·rHDL (blue), with a Stokes diameter of ≈ 11 nm.

reagents (***Fig. 2-4***). Although extensive crosslinking occurred when Cy3-β_2AR was reconstituted in phospholipid vesicles very little crosslinking was observed in detergent micelles, implying that receptors are not proximate enough (using either 12Å or 24Å crosslinkers) to be crosslinked in detergent micelles. The homogeneity and monodispersion are important properties of these preparations that are relevant to TIRF

a

	Cy3-β_2AR	Cy3-β_2AR-rHDL	Cy5-β_2AR	Cy5-β_2AR-rHDL
1 label	38.2 %	48.9 %	42.1 %	56.3 %
2 labels	27.7 %	31.6 %	37.2 %	33.6 %
3 labels	8.5 %	3.4 %	5.3 %	2.1 %
Not countable	25.6 %	16.1 %	15.4 %	8.0 %

b

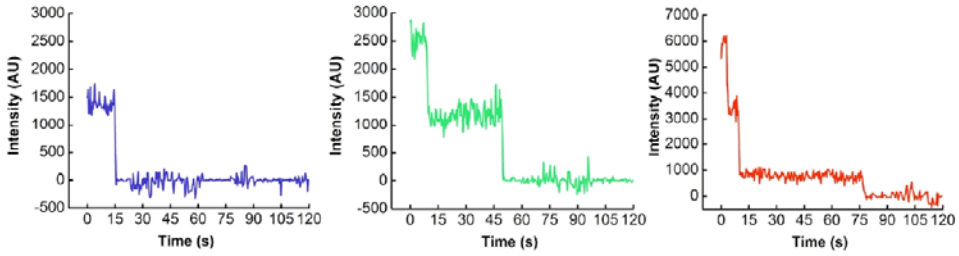

Figure 2-3. Labeling efficiency of β_2AR estimated by TIRF imaging and photobleach-step counting. **(a)** The percentage of receptors containing one, two, or three fluorescent labels was determined by manually counting the number of photobleach steps in the intensity time trace for at least 400 individual receptors or rHDL particles. In each case it was impossible to count photobleach steps for a fraction of molecules due to either low signal-to-noise or fluorophore blinking. **(b)** Illustrative time traces for molecules counted as containing one, two, or three fluorescent labels. To achieve quantitative labeling, preparations of β_2AR were labeled with cysteine-reactive derivatives of Cy3 or Cy5 at a stoichiometry of 20 fluorophores to one receptor molecule. From absorption spectra we estimate that between 1.6 and 2.5 mol of fluorophore were incorporated per mole of β_2AR under these conditions. Over 35% of Cy3-and Cy5-β_2AR molecules were observed to contain multiple fluorophores, as determined by counting the number of photobleaching events for individual receptors imaged by TIRF (e.g., Cy3-β_2AR, 28% double-labeled, 9% triple-labeled; Cy5-β2AR, 37% double-labeled, 5% triple-labeled). To estimate the fraction of unlabeled β_2AR in such a sample, we simulated the labeling kinetics of the three most reactive cysteines using a mathematical model (see Materials and Methods). This model was able to accurately reproduce the observed fractions of double-and triple-labeling. Based on our most conservative estimate from this model, a maximum of 0.4% of β_2AR remains.

imaging and FRET analysis below.

Preparations of Cy3- and Cy5-β_2AR were reconstituted into rHDL and resolved by size exclusion chromatography. Both Cy3- and Cy5-β_2AR•rHDL elute as a uniform absorbance peak (***Fig. 2-2c***) with a Stokes' diameter of 11 nm (as determined by protein standards), slightly larger than the diameter for empty discs alone (~10.5 nm, not shown). This small difference, likely due to the extra-membrane loops and termini of the receptor,

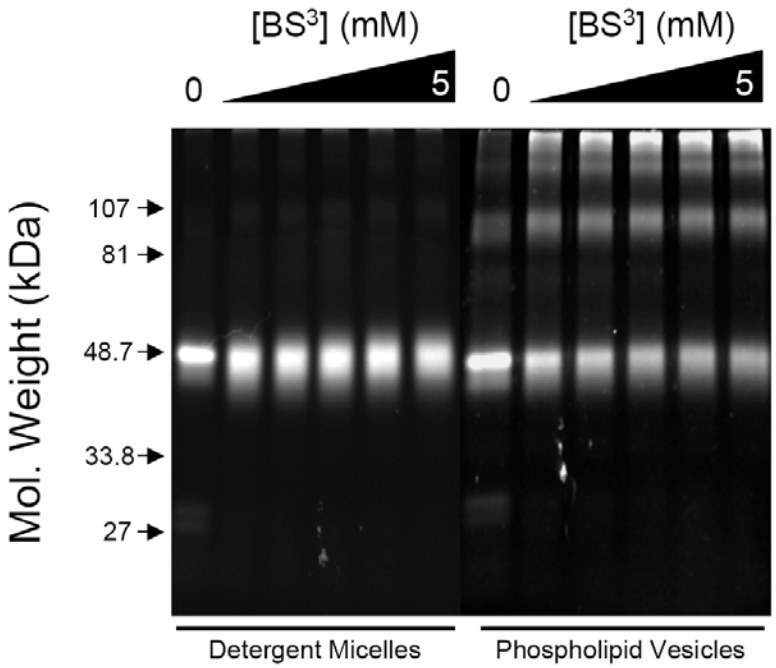

Figure 2-4. Purified β_2AR in DDM micelles is monomeric before reconstitution in vesicles. To ensure that the Cy3-or Cy5-labeled β_2AR is not oligomeric before rHDL reconstitution (i.e., in detergent micelles), cross-linking analysis with BS^3 (11.4-Å spacer; Pierce) was performed. Although considerable intramolecular cross-linking (band spreading) was observed, no detectable intermolecular cross-linking was observed in Cy3 β_{2A}R in detergent micelles. These data suggest that there are insignificant levels of oligomeric receptor complexes in detergent micelles. In contrast, incubation of phospholipid vesicle-reconstituted β_2AR with BS^3 resulted in the concentration-dependent appearance of higher-order species, including dimers, and what appear to be aggregates near the top portion of the separating gel. Cy3-labeled β_2AR (1 μM) in detergent micelles (0.1% DDM) or reconstituted in phospholipid vesicles was incubated in the absence or presence of increasing concentrations of BS^3 for 60 min on ice. The reaction was terminated with 20 mM Tris-HCl, pH 8.0. Samples were resolved by SDS-PAGE and imaged on a UV gel documentation station (FluorChem 8800, Alpha Innotech) using rhodamine/Texas red filters. Similar results were obtained using an amine cross-linker with a longer linker, *Bis*(NHS)PEO_5 (21.7-Å pegylated spacer; Pierce, data not shown). Phospholipid reconstitution into DOPC:cholesterol vesicles was performed as described in the *Materials and Methods*.

demonstrates that incorporation of β_2AR does not perturb the structure or stability of the rHDL particle. Fractions representing the chromatogram peak were isolated and used for TIRF and fluorescence resonance energy transfer (FRET) analysis (marked with an asterisk ***Fig. 2-2c and inset***). These fractions represent both the peak in fluorescence intensity and also [^{3}H]DHAP binding activity (illustrated for Cy3-β_2AR•rHDL).

TIRF imaging of either Cy3-β_2AR•rHDL (***Fig. 2-5a***) or Cy5-β_2AR•rHDL (***Fig. 2-5b***) reveals discrete, monodisperse fluorescent particles. Subtle variability in intensity is due to incorporation of multiple fluorophores per molecule of β_2AR (See step photobleaching in the ***Fig. 2-3b***). When equal amounts of Cy3-β_2AR•rHDL and Cy5-β_2AR•rHDL were mixed together and imaged, only 1.8 ± 0.6% displayed colocalization (average ± s.e.m. of 10 images, total of 1916 molecules, ***Fig. 2-5c&f***. Strikingly, when equal amounts of Cy3-β_2AR and Cy5-β_2AR receptors were mixed prior to reconstitution in HDL, only 2.3 ± 0.6% of Cy3 and Cy5 labeled receptors colocalized (10 images containing a total of 2022 receptors, ***Fig. 2-5d&f***. The degree of colocalization of these fluorophores is not different than mixtures of Cy3-β_2AR•rHDL and Cy5-β_2AR•rHDL (***Fig. 2-5f***) nor different than TIRF imaging of Cy3-β_2AR or Cy5-β_2AR in detergent micelles (data not shown**)**. Both percentages are highly statistically different from a positive control for colocalization (double-labeled Cy3-Cy5-β_2AR, 44 ± 2% of which were colabeled, i.e. fluoresced in both the Cy3 and Cy5 channels, ***Figs. 2-3e, 2-4a***). These data strongly support the notion that under the conditions used for reconstitution, each HDL particle contains only a single, monomeric β_2AR molecule.

Single-molecule experiments were confirmed by ensemble fluorescence resonance energy transfer (FRET) measurements to assess the relative physical distance

between Cy3- and Cy5-labeled receptors incorporated into rHDL. Since the inner diameter of rHDL (~85 Å) is close to the Förster distance for Cy3 and Cy5 (~60 Å), FRET should only occur from Cy3- to Cy5-labeled receptors within the same rHDL particle. However, no FRET was observed from rHDL particles formed from a mixture of Cy3-β_2AR and Cy5-β_2AR under conditions described above (***Fig. 2-6b***). In fact, the emission scan of this preparation remained unchanged when resolubilized in 1% DDM, and was comparable to emission spectra of Cy3-β_2AR and Cy5-β_2AR mixed together in detergent micelles (***Fig. 2-6c***).

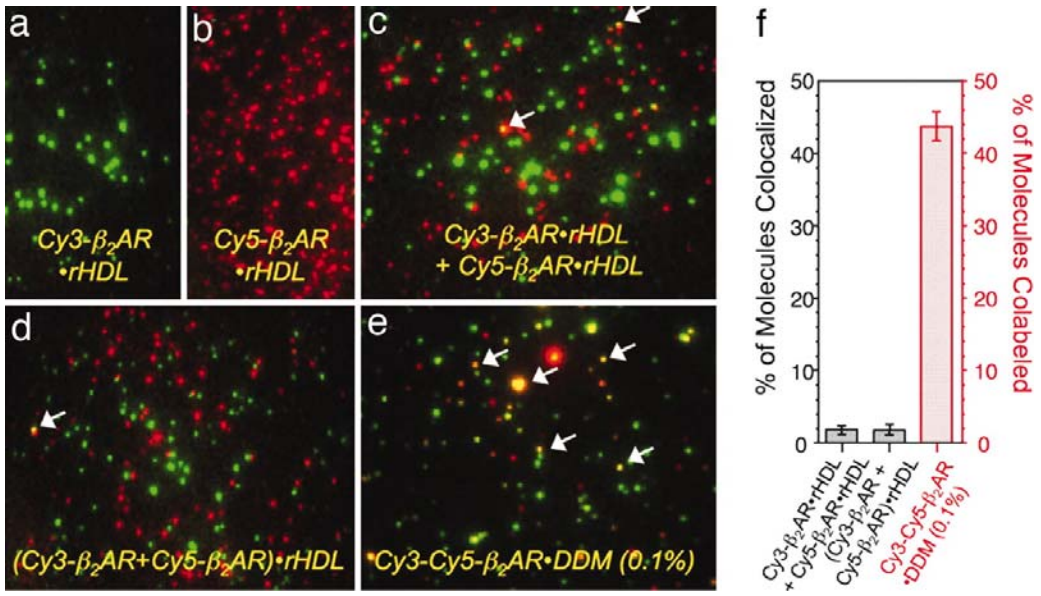

Figure 2-5. TIRF of Cy3- and Cy5-labeled β_2AR in rHDL reveals that the vast majority of β_2AR are monomeric. Conditions for the reconstitutions illustrated are: **(a)** Cy3-β_2AR·rHDL and **(b)** Cy5-β_2AR·rHDL particles alone, or **(c)** Cy3-β_2AR·rHDL and Cy5-β_2AR·rHDL mixed together at equal concentrations, **(d)** Cy3-β_2AR and Cy5-β_2AR mixed together at equal concentrations before reconstitution (Cy3-β_2AR + Cy5-β_2AR)·rHDL, **(e)** β_2AR colabeled with Cy3 and Cy5 in 0.1% DDM, and **(f)** bar graph summarizing TIRF data in **c–e**. Cy3- and/or Cy5-labeled receptors were reconstituted in rHDL at a β_2AR:ApoA-I ratio of 1:100 (β_2AR:rHDL ratio of 1:50) in the presence of POPC/POPG and resolved by SEC. Receptor concentrations were maintained at 1 μM. Fractions were analyzed by TIRF as described in *Materials and Methods*.

In contrast, FRET was observed when Cy3-β_2AR and Cy5-β_2AR were reconstituted in phospholipid vesicles (i.e., in the absence of apoA-I, ***Fig. 2-6a***), suggesting that these receptors are oligomeric. The addition of 1% DDM to the

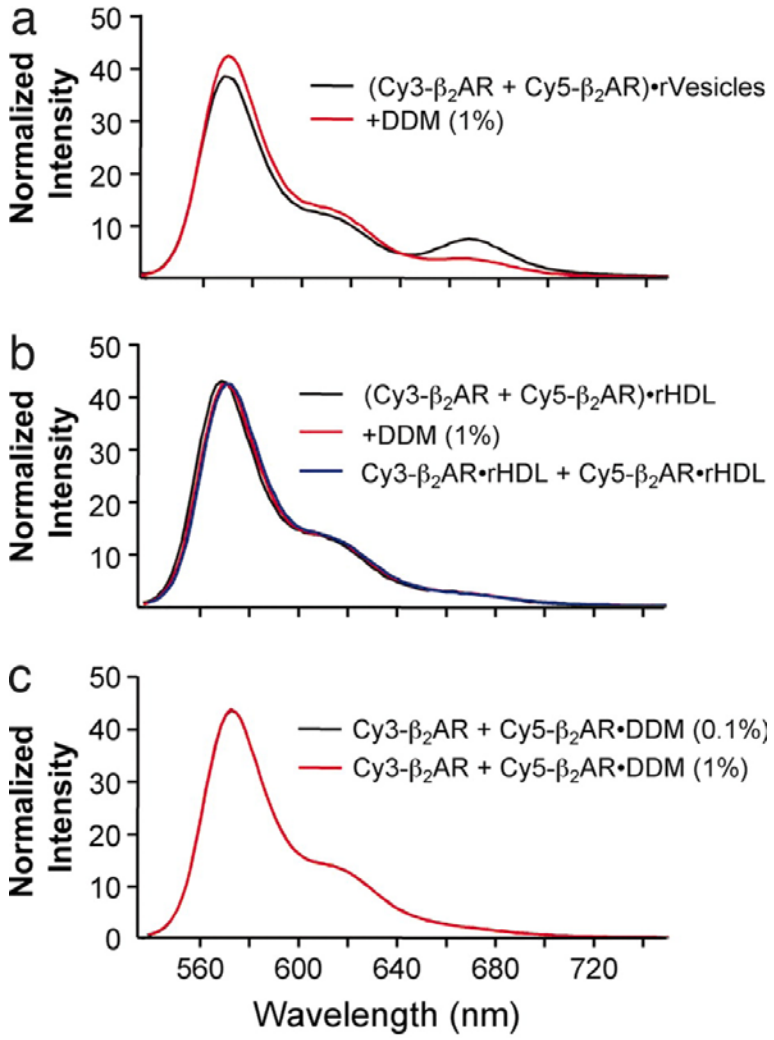

Figure 2-6. FRET measurements confirm monomeric β_2AR in rHDL. Cy3- and Cy5-labeled β_2AR preparations were reconstituted under different conditions, and normalized spectra were analyzed for the presence of FRET, as indicated by increased acceptor (Cy5) emission (at 670 nm) and the concomitant decrease in donor (Cy3) emission (at 575 nm). **(a)** Equal amounts of Cy3-β_2AR and Cy5-β_2AR were mixed and reconstituted into phospholipid vesicles (rVesicles). (Cy3-β_2AR + Cy5-β_2AR)·rVesicles display FRET, which is reduced on exposure to 1% DDM (red), a detergent concentration that disrupts and resolubilizes the vesicles. **(b)** In contrast, no significant FRET is observed in (Cy3-β_2AR + Cy5-β_2AR)·rHDL in the absence (black) or presence (red) of 1% DDM. These spectra are identical to spectra obtained from equal mixtures of Cy3-β_2AR·rHDL and Cy5-β_2AR·rHDL (blue). **(c)** Normalized spectra are also identical to mixtures of Cy3-β_2AR and Cy5-β_2AR in DDM micelles at 0.1% DDM (black) or at 1% (red).

vesicles markedly reduced the FRET due to oligomerization (***Fig 6a***). As mentioned earlier, oligomerization in vesicles was also detected by crosslinking studies with bifunctional amine crosslinkers (***Fig. 2-4***). Taken together these data demonstrate that rHDL particles represent a unique experimental system for studying monomeric GPCRs in a phospholipid environment.

Monomeric β2AR in rHDL functionally couples to G proteins. Monomeric β_2ARs in rHDL couple efficiently to the purified stimulatory heterotrimeric G protein Gs, as shown in ***Fig. 2-7***. Isoproterenol promotes rapid guanine nucleotide exchange on Gs reconstituted into CFP-β_2AR•rHDL particles (50 fmol receptor, ***Fig. 2-7a***). [^{35}S]GTPγS binding appears biphasic with a B_{max} of ~60 ± 10 fmol. In contrast, [^{35}S]GTPγS binding in the presence of timolol (an inverse agonist) occurred in a slow but saturable manner within 15 min and with an estimated B_{max} of 33.5 fmol. The difference between these binding conditions yields the isoproterenol-β_2AR-specific [^{35}S]GTPγS binding component of 26.5 fmol and represents approximately 45 ± 7% of the total [^{35}S]GTPγS binding. The isoproterenol-specific stimulated [^{35}S]GTPγS binding yields a final R:G ratio of 50 fmol:26.5 fmol or approximately 1:0.53. These data suggest that up to 53% of the β_2AR•rHDL particles may contain a single G protein. There is a possibility that multiple G proteins may be reconstituted per receptor-containing particle, however, steric crowding owing to the physical dimensions of the Gsαβγ heterotrimer (>80 Å from tip to tip) suggests that this is unlikely to occur.

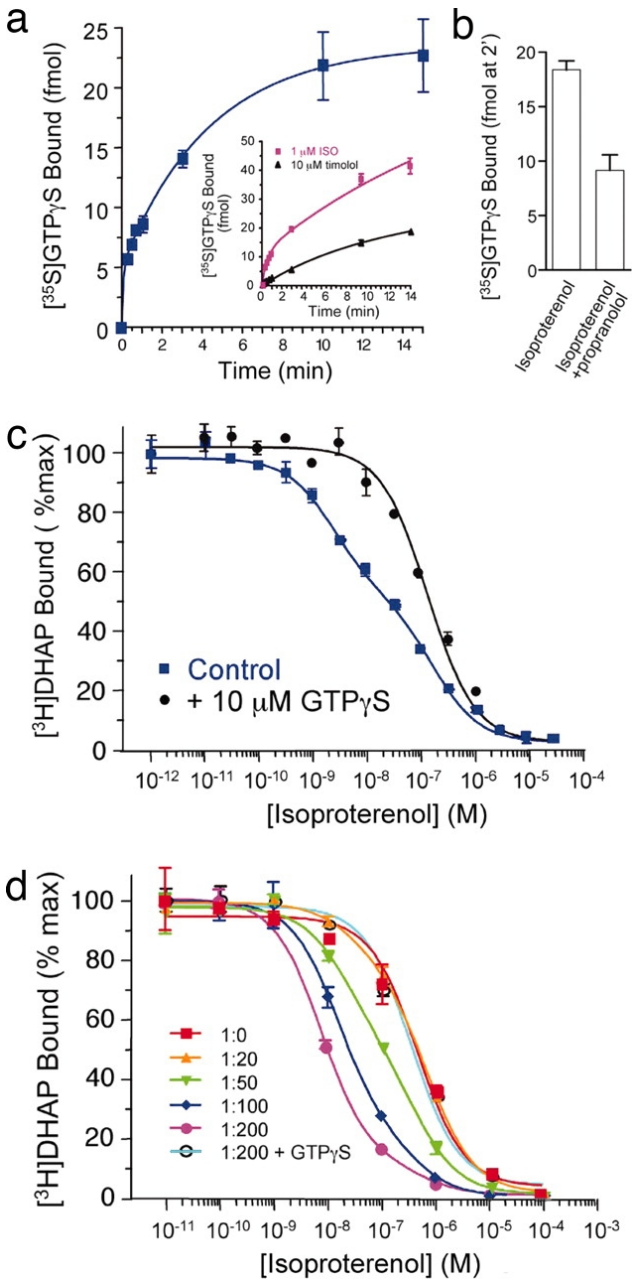

Figure 2-7. Monomeric β_2AR incorporated in rHDL particles couples efficiently to G proteins. **(a)** ISO-induced [^{35}S]GTPγS binding to monomeric-β_2AR·Gs·rHDL particles. β_2AR·Gs·rHDL particles were preincubated with either 1 μM ISO (magenta) or 10 μM timolol (black) in the presence of 100 nM [^{35}S]GTPγS and 2 mM $MgCl_2$ to stimulate [^{35}S]GTPγS binding **(Inset)**. Aliquots (at times indicated) were removed, and binding was terminated with a quench buffer. Agonist-specific [^{35}S]GTPγS binding to β_2AR·Gs·rHDL particles (blue) represents the difference between ISO-stimulated and timolol-bound data (*Inset*). **(b)** Propranolol inhibition of ISO-stimulated [^{35}S]GTPγS binding. β_2AR·Gs·rHDL particles were preincubated with either 1 μM ISO or 1 μM ISO plus 3 mM propranolol and then assayed for [^{35}S]GTPγS (2 min at 30°C), as above. **(c)** High-affinity ISO inhibition of [^{3}H]DHAP binding to monomeric β_2AR in rHDL occurs in the presence of G proteins (blue) but is abolished by coincubation of 10 μM GTPγS (black).

The K_{high} (8.0 ± 2.4 nM) and K_{low} (360 ± 110 nM) sites represent 56% and 44% of total binding, respectively. Purified Gs was added to preformed β_2AR·rHDL particles at a final R:G ratio of 1:0.53, as determined by [^{35}S]GTPγS binding and described in *Materials and Methods*. **(d)** Increasing the concentration of Gs and thus the R:G ratio (e.g., R:G of 1:200) increases the proportion of high-affinity agonist sites to > 90%. Note that the 1:200 represents the initial R:G ratio and not the final functional R:G (see text). Coincubation with 10 μM GTPγS to the 1:200 reconstitution condition completely abolishes the high-affinity ISO binding (open circles), yielding a K_i similar to the K_{low}. These data were fit with a nonlinear regression (***c*** and ***d***) or two-phase exponential fit using Prism 4.0 (***a***) (GraphPad).

When fit to a two-phase exponential association curve, [^{35}S]GTPγS binding data also reveal an initial rapid burst of binding with a halftime of < 10 s, followed by a slower rate with a halftime of 4.3 ± 1.3 min. The initial burst, not observed in the presence of timolol, is consistent with [^{35}S]GTPγS binding to empty Gs (devoid of GDP) and represents a pre-coupled G protein-receptor complex [72-74]. The slower phase is likely due to the inability of inverse agonists to completely inhibit basal receptor activation [75]. The inability of the inverse agonist to completely reduce the basal receptor may slightly underestimate the isoproterenol-stimulated component of [^{35}S]GTPγS binding. It should also be noted that although high amounts of G protein are required in the initial reconstitution (R:G ratio of 1:50), very low amounts of G protein actually incorporate into the receptor containing particles. The vast majority of G proteins aggregate and precipitate due to the absence of detergent, a requirement to keep the acylated (Gsα) and prenylated (Gγ) subunits of the heterotrimeric G protein in solution.

Monomeric β_2AR also undergoes allosteric modulation of agonist binding by G proteins. Analysis of isoproterenol inhibition of [^{3}H]DHAP binding to these preparations reveals a classic biphasic competition curve with an observed K_{high} of 8.0 ± 2.4 nM and a K_{low} of 0.36 ± 0.11 μM (n=5) (***Fig. 2-7b***), in good agreement with previously reported

values [76]. The functional uncoupling of Gs by GTPγS yielded a monophasic inhibition curve with a K_i of 0.13 ± 0.09 μM (n=2), very similar to the K_{low} value. The high-affinity isoproterenol sites (K_{high}) represented 57 ± 4% (n=5) of the total [^{3}H]DHAP binding, remarkably close to the proportion of receptors that contain G proteins (53% from [^{35}S]GTPγS binding). The fraction of high-affinity isoproterenol sites increases in a G protein concentration-dependent manner to levels approaching 90% when the final R:G ratio is approximately 1:2 (***Fig. 2-7c***). This ratio was estimated from the fractional survival of Gsαβγ remaining following the deleterious reduction in detergent concentration to levels well below the CMC during the reconstitution procedure (as described earlier) and the amount of β_2AR in the assay (50 fmol).

Discussion

Although GPCRs may exist as oligomers, as evident in imaging studies from native membranes [10], modeling studies, and FRET/BRET experiments [62-64], our study shows that the minimal functional unit is unequivocally a monomer. Agonist activation of monomeric receptors induces rapid guanine-nucleotide exchange in G proteins. G proteins directly induce the monomeric receptor to adopt a conformation that binds agonist with high affinity (nM) compared to conditions where G proteins are absent or uncoupled (μM). These data resolve a highly controversial question at the core of GPCR signal transduction. While the β_2AR is only one of several hundred GPCRs in the genome, it is likely that the observations reported here can be generalized to at least the class A, or rhodopsin-like receptors. Members of this family encompass most of the hormone receptors that are targeted by clinically useful therapeutics. Thus, elucidating

their minimal functional oligomeric state is critical for understanding their mechanism of action.

One of the earliest reports providing evidence that GPCRs may exist as dimers in the plasma membrane was published in 1996 [23] and was met with some criticism by investigators in the field. However, since that study, which used the β_2AR as a model system, there have been a growing number of reports documenting both homo- and heterodimerization of GPCRs using a variety of techniques [10, 26, 27, 77-79]. Consequently, the existence of GPCR dimers is now widely accepted. Studies documenting the requirement for heterodimerization in $GABA_B$ receptor signaling as well as studies providing evidence that dimerization is required for efficient export of GPCRs from the endoplasmic reticulum have led to speculation that a dimer is likely to be the functional unit for GPCR signal transduction [78]. However, rigorous analysis of the role of dimers in G protein activation has previously not been possible because of the inability to physically isolate and characterize the function of a monomeric GPCR embedded in its membrane milieu.

In this study, we incorporate purified β_2AR into rHDL particles along with purified Gs heterotrimer. We demonstrate that the detergent-solubilized and purified β_2AR is monomeric before reconstitution, and that the rHDL particles contain only a single β_2AR. Our study shows that the minimal functional unit is a monomer by virtue of the fact that agonist treatment induces rapid guanine-nucleotide exchange in G proteins. Moreover, G proteins directly induce the monomeric receptor to adopt a conformation that binds agonists with high affinity (nanomolar) compared with conditions where G proteins are absent or uncoupled (micromolar). By increasing the proportion of β_2AR

occupied by G proteins, we observe an increase in the proportion of high-affinity agonist-binding sites. These data represent direct support of the original "ternary complex" coined by DeLean *et al.* approximately 30 years ago [7] and refutes the contributions of receptor oligomers toward high-affinity agonist binding.

The data presented here do not refute that receptors exist as oligomers in membranes, but rather the data suggest that oligomerization may play a minor role in G protein activation. In fact, the data remain consistent with a pentameric receptor–G protein complex model (R:R:Gα:Gβ:Gγ), as has been proposed for the $GABA_B$ receptor, mGluR, and rhodopsin [34, 58, 80]. In this model, only one of the two receptors within the dimer is capable of coupling to the G proteins.

Cumulatively, these data resolve a highly controversial question at the core of GPCR signal transduction. Although the β_2AR is only one of several hundred GPCRs in the genome, it is likely that the observations reported here can be generalized to at least the class A or rhodopsin-like receptors. Members of this family encompass most of the hormone receptors that are targeted by clinically useful therapeutics. Thus, elucidating their minimal functional oligomeric state is critical for understanding their mechanism of action.

Materials and Methods

Materials. G protein baculoviruses encoding $G\alpha_s$, his6-$G\beta_1$ and $G\gamma_2$ were generously provided by Dr. Alfred G. Gilman (UT Southwestern). Expired human serum was generously donated by Dr. Bert La Du (University of Michigan). All lipids were purchased from Avanti Polar Lipids (Alabaster, AL). DDM was obtained from Dojindo

Molecular Technologies (Gaithersburg, MD). Sodium cholate was purchased from Sigma. (±)-alprenolol, S(-)-timolol, (±)-propranolol, and (-)-isoproterenol were obtained from Sigma (St. Louis, MO). [^{3}H]Dihydroalprenolol and [^{35}S]GTPγS were obtained from Perkin Elmer (Foster City, CA). Cy3 and Cy5 maleimide were purchased from GE Healthcare (Piscataway, NJ). All other reagents were of analytical grade.

Buffers. Buffer A: 50 mM Tris-HCl pH 8, 50 mM NaCl, protease inhibitors (PIs: 34 mg/ml each of L-tosylamido-2-phenylethyl chloromethyl ketone, 1-chloro-3-tosylamido-7-amino-2-heptanone and phenylmethylsulfonyl fluoride, and 3 mg/ml each of leupeptin and lima bean trypsin inhibitor). Buffer B: 50 mM Tris-HCl pH 8, 50 mM NaCl, PIs. Buffer C: 20 mM Hepes pH 8, 1 mM EDTA, 0.1% DDM, PIs. Buffer D: 50 mM Tris-HCl pH 8, 1 mM $CaCl_2$, 3 M NaCl, 5 μM EDTA. Buffer E: 20 mM Tris-HCl pH 8, 1 mM $CaCl_2$, 5 μM EDTA, 0.1% Triton X 100. Buffer F: 25 mM K-acetate pH 5, 1 mM EDTA, 0.1% Triton X-100. Buffer G: 20 mM Hepes pH 8, 100 mM NaCl, 1 mM EDTA. Buffer H: 20 mM Hepes pH 7.5, 100 mM NaCl. Buffer I: 100 mM NaCl, 20 mM Hepes pH 7.5, 0.1% dodecylmaltoside (Anatrace). Buffer J: Buffer I and 1 mM EDTA. Buffer K: Buffer I with 300 μM alprenolol (Sigma) and 1 mM $CaCl_2$. Buffer L: Buffer I with 1 mM $CaCl_2$. Buffer M: Buffer I with 0.01% cholesterol hemisuccinate.

Receptor purification and labeling. β_2AR (WT or CFP-fused) was expressed in Sf9 cells and solubilized using methods previously described [81]. For CFP-β_2AR: DDM-solubilized extract was applied to a metal-chelate affinity column (Talon, Clontech). Samples were washed with Buffer B + 0.1% DDM with 2.5 mM imidazole and then subsequently eluted with Buffer B with 100 mM imidazole, 0.1% DDM. Peak fractions were applied to a 1 ml Source Q anion exchange column (GE Healthcare) in

Buffer C. CFP-β_2AR was eluted with a 15 ml 0-40% linear gradient with Buffer C + 1 M NaCl. Peak fractions were pooled and resolved on a Superdex 200 size exclusion column in Buffer C + 50 mM NaCl to resolve the CFP-β_2AR from the clipped CFP. The resultant CFP-β_2AR is greater than 95% pure and stored on ice until use. For wt-β_2AR: $CaCl_2$ was added to the DDM-solubilized extract to a final concentration of 1 mM and the detergent solubilized β2AR was purified by M1-Flag affinity chromatography (Sigma). The receptor was eluted from the M1-Flag resin in Buffer J. The concentration of functional, purified receptor was determined using a saturating concentration (10 nM) of [^{3}H]dihydroalprenolol as previously described [81]. Flag-purified receptor was then purified by alprenolol-Sepharose chromatography as described [81]. The receptor was eluted from alprenolol-Sepharose with Buffer K and loaded directly onto M1-Flag resin. The M1-Flag resin was washed with Buffer I to remove free alprenolol and eluted with Buffer J. Two liters of Sf9 cells typically yield 500 μl of a 5 μM solution of β_2AR.

Purification of human apoA-I: WT human apoA-I was purified from human serum by a protocol adapted from Gan *et al.* [82]; all procedures were performed at room temperature (RT) unless noted. Frozen serum (-20°C in 10 mM $CaCl_2$) was thawed at 37°C, strained through cheesecloth, and then centrifuged at 5,000 x *g* for 10 min to pellet any debris. This clarified serum was then made up to the following buffer condition: Buffer D. This solution was combined with equal serum volume of blue agarose resin (Cibacron blue F3GA-agarose, Sigma) equilibrated in Buffer D, and stirred for 30 min. Resin was then washed by filtering through a Whatman #1 filter in a Büchner funnel. The resin cake was then resuspended in 3 x resin volume Buffer D and then re-filtered. The resin was washed (3-4 times), until absorbance at 280 nm of the filtrate was less than

0.025. The resin was washed twice more in the same manner with Buffer D without 3 M NaCl. After the last wash, the cake was resuspended in an equal volume of the same buffer and loaded onto an empty column. The remaining bound proteins were then eluted with the same buffer + 5 mM cholate. ApoA-I was typically 80-90% pure at this stage. To delipidate the apoA-I, fractions were pooled and concentrated using an Amicon stirred ultrafiltration cell affixed with a 10,000 MWCO filter (Millipore) and then diluted 1:1 in 25 mM Tris-HCl pH 8, 1 mM $CaCl_2$, 5 mM EDTA, 0.2% Triton X-100. This was then applied to a 70 ml Q Sepharose (Amersham Pharmacia) column equilibrated in Buffer E and eluted with a shallow linear gradient with Buffer E + 1 M NaCl, apoA-I usually eluted around 10-15%. The remaining contaminants were removed using a SP Sepharose (Amersham Pharmacia) column (70 ml) equilibrated in Buffer F and eluted with a linear gradient against Buffer F + 1 M NaCl. To exchange the Triton X-100 for cholate, SP Sepharose fractions were applied to a Superdex 200 size exclusion column (Amersham Pharmacia) in Buffer G + 20 mM cholate, at 4°C. ApoA-I fractions were pooled and concentrated to at least 10 mg/ml, then dialyzed at 4°C against Buffer G + 5 mM cholate and stored at -80°C until further use.

***In vitro* reconstitution of rHDL.** High-density lipoproteins were reconstituted *in vitro* according to a protocol adapted from Jonas [50]. Briefly, DMPC and POPC, were used alone, or as a mixture of POPC and POPG in combination (3:2 molar ratio), to mimic the zwitterionic environment of a cell membrane [40]. A typical rHDL reconstitution consisted of the following components: 24 mM detergent (cholate or DDM), 8 mM lipids, and 100 μM apoA-I. Lipids were solubilized with a solution of 20 mM Hepes pH 8, 100 mM NaCl, 1 mM EDTA + 50 mM detergent. To reconstitute

receptors, purified apoA-I was added to at least 10-fold excess ([apoA-I]:[receptor]) to receptor preparations diluted in solubilized lipids. Following an incubation of 1-2 hrs at the Tm of the lipid combination, samples were added to an equal volume of hydrated BioBeads (BioRad) for an additional 1-2 hrs to remove detergents, resulting in the formation of rHDL particles. Samples were stored on ice until used. If necessary, β_2AR•rHDL particles were separated from receptor-free rHDL by M1-anti-FLAG immunoaffinity chromatography. Purified β_2AR•rHDL particles were eluted with EDTA (10 mM) and stored on ice until further use.

Negative staining and transmission electron microscopy of rHDL particles. rHDL samples were placed on a carbon-coated copper grid and stained with 1 % phosphotungstic acid, pH 6.5. Samples were imaged in a Philips CM-100 transmission electron microscope operating at 60 kV.

Analytical size exclusion chromatography. Analytical size exclusion chromatography was performed on a HR10/30 column (Amersham) Superdex 200 (Amersham) using the BioLogic DuoFlow system (BioRad) at 4º C. Fractions from the column (200 μL) were collected in a 96-well plate for further analysis. Cy3 fluorescence (λ_{ex}=544 nm, λ_{em}=595 nm) was analyzed in a Victor^2 ™ fluorescence plate reader (Perkin Elmer). The column was calibrated with thyroglobulin [669 kDa, Stokes diameter (Sd) = 17.2 nm], apoferritin (432 kDa, Sd = 12.2 nm), alcohol dehydrogenase (150 kDa, Sd = 9.1 nm), BSA (66 kDa, Sd = 7.2 nm), carbonic anhydrase (29 kDa, Sd = 4 nm).

Cy3 and Cy5 labeling of β_2AR. Purified β_2AR (5 μM) was labeled with cysteine-reactive Cy3-maleimide (100 μM) or Cy5-maleimide (100 μM, GE Healthcare) for 60 min at 25 °C in Buffer H + 0.1% DDM in the presence of Tris(2-carboxyethyl)

phosphine hydrochloride (200 μM). The β_2AR samples were incubated with iodoacetamide (2 mM) for 30 min to alkylate unlabeled cysteines and to prevent the formation of disulfide-linked oligomers in detergent solution. The conjugation reactions were quenched by cysteine (2 mM). Labeled protein (Cy3-β_2AR or Cy5-β_2AR) was separated from free dye and iodoacetamide by gel filtration (Sephadex G-50 Fine). The efficiency of labeling (stoichiometry) was estimated from UV-Vis absorption spectra, using the following extinction coefficients [44]: ε554, Cy3 = 150,000 M^{-1} cm^{-1}, ε652, Cy5 = 250,000 M^{-1} cm^{-1}, and ε280, β_2AR = 116 mM^{-1} cm^{-1}. The receptor extinction coefficient at 280 nm was estimated from a standard dilution curve of purified β_2AR for which the concentration was determined by saturation radioligand binding. The contribution of fluorophore absorbance at 280 nm was subtracted (8% of the absorbance at 554 nm for Cy3, and 5% of the absorbance at 652 nm for Cy5, CyDye mono-reactive (NHS esters handbook, GE Healthcare)). To prepare the dual-labeled positive control for colocalization, a portion of Cy3-β_2AR (2 μM) was labeled by incubation with the amine reactive dye Cy5-mono-NHS-ester (400 μM, GE Healthcare) for 3 h at 25 °C. Labeled protein (Cy3-Cy5–β_2AR) was separated from free dye by gel filtration.

Single-molecule imaging. Single-molecule imaging was performed on an in-house, custom-designed total internal reflection fluorescence (TIRF) microscope based on a Nikon TE2000-U inverted microscope using a standard through-the-objective configuration [83]. A 532 nm green diode-pumped, frequency-doubled Nd:YAG laser (for Cy3 excitation, Compass 215M, Coherent, Santa Clara, CA) and a 638 nm red diode laser (for Cy5 excitation, RCL-638-025, Crystalaser, Reno, NV) were used as the excitation sources. Lab-Tek II chambered coverglasses (Nalgene Nunc International,

Rochester, NY) were used to contain and image all samples. To image a sample, 500 μL of ~10 pM β_2AR•rHDL was added to the chamber to allow nonspecific adsorption to the glass surface. After a 5 min incubation, the protein solution was pipetted off and immediately replaced by 500 μL PBS (Gibco) to stop adsorption of additional molecules from solution. Images of Cy5 and Cy3 were acquired sequentially, with WinView (Roper Scientific), by switching the excitation laser and the emission band pass filter. The excitation power density was 48.8 W/cm2 for the green laser and 22.4 W/cm2 for the red laser. The integration time of the CCD camera was 0.4 sec per frame. To avoid the possible masking of Cy3 fluorescence due to energy transfer from Cy3 to Cy5, 200 frames were acquired in the Cy5 channel before acquisition of the Cy3 image to ensure that all Cy5 molecules are photobleached.

Images were analyzed with an in-house, custom-designed program. In a fluorescent image, each local maximum exceeding a certain height threshold was fitted with a two-dimensional Gaussian function in a 7 pixel x 7 pixel area around it. A fluorescent molecule was identified if the fitted results satisfied both the height and width criteria. The fluorescence time trace of a molecule is obtained by identifying the molecule in the first frame of an image stack and then fitting each subsequent frame with a two-dimensional Gaussian function. The fraction of colocalized molecules was calculated as: 2*(no. colocalized spots) / (no. Cy3 spots + no. Cy5 spots) where a Cy3 or Cy5 spot is classified as any fluorescent molecule as described above, and assuming that a colocalized spot contains two receptors. The fraction of colabeled molecules for the dual-labeled Cy3-Cy5-β_2AR sample was calculated as: (no. colocalized spots) / (no. Cy3 spots + no. Cy5 spots – no. colocalized spots).

Ensemble FRET spectra. Steady-state FRET measurements were determined on a Spex FluoroMax-3 spectrofluorometer (Horiba Jobin Yvon, Inc.) with photon-counting mode at 25º C. Spectra were collected as follows: Cy3 emission (λ_{ex}=525 nm, λem=535 to 751 nm), Cy5 emission (λ_{ex}=625 nm, λem=635 to 751 nm).

Saturation radioligand-binding assays. Binding reactions were prepared in 100 µl volumes in 96-well plates. Samples were incubated with various concentrations of β_2AR antagonist [^{3}H]dihydroalprenolol ([^{3}H]DHAP) (0.1-46 nM) in 50 mM Tris-HCl pH 8, 150 mM NaCl (TBS) [or TBS with 1% detergent (DDM or cholate) for detergent-solubilized binding]. Nonspecific binding was determined in the presence of 20 mM propranolol. Membrane samples were incubated for 90 min at RT. Detergent-solubilized, purified samples were incubated for 60 min at 30°C for saturation isotherms, or for 30 min at 30°C for single point saturation binding. For separating free [^{3}H]DHAP from bound, membrane samples were filtered on glass fiber filter plates and detergent solubilized samples were filtered on gel filtration columns. For the rHDL samples, both methods were used successfully, although the glass fiber plates retained only about 80% of the binding seen on the gel filtration columns.

For glass fiber filtering, GF/B 96-well filter plates (Whatman) were used in conjunction with a vacuum manifold. Wells were prewet with TBS. Samples were applied and washed 3x with 200 ml of TBS. Scintillation mixture was added (Microscint 0, Packard) and plates were counted on a TopCount scintillation counter (Packard). For gel filtration, samples were applied to Sephadex G-50 columns equilibrated in TBS (or TBS + 0.05% DDM or 0.5% cholate). Scintillation mixture (Cytoscint, MP Biomedicals) was added to the flowthrough fractions (containing the bound receptor) and counted on a

Beckman LS5000. Specific binding was determined by subtracting nonspecific binding from total binding.

G protein reconstitution: Purified G_s [84] (stored in 11 mM CHAPS) was reconstituted into preformed impure β_2AR•rHDL particles (containing excess empty rHDL particles) at an initial R:G ratio of 1:50. Concentrated G_s stocks were added such that the CHAPS was diluted at least 700-fold to reduce the CHAPS concentration to well below the CMC (6-10 mM). This had no effect on the integrity of the particles, as assessed by size exclusion chromatography (data not shown). Treatment of G_s-reconstituted samples with BioBeads, to remove trace amounts of CHAPS, before gel filtration chromatography had no effect on the results.

Agonist competition assays: Agonist competition assays were performed on G protein-reconstituted samples under similar conditions as used in the saturation binding assays except that a fixed concentration of [^{3}H]DHAP (2 nM) was competed with various concentrations of isoproterenol ($1x10^{-12}$ – $1x10^{-4}$ M), with or without the addition of 10 mM GTPγS. Binding reactions contained 0.02% ascorbic acid to prevent oxidation of the isoproterenol. Samples were incubated for 30 min at 30°C and then filtered on glass fiber plates as above. Normalized data were fit to a two-site competition binding model using Prism (GraphPad).

GTPγS-binding assay: G protein reconstitution was performed as above. Agonist-stimulated [^{35}S]GTPγS-binding assays were performed essentially as described by Asano *et al.* [85]. Receptor samples were combined with either 1 mM isoproterenol, 10 mM timolol, or 1 mM isoproterenol plus 3 mM propranolol in buffer comprised of Buffer H plus 2 mM $MgCl_2$ and 0.02% ascorbic acid. These were allowed to preincubate

at 30°C for 5 min before being combined with 100 nM isotopically diluted [^{35}S]GTPγS. Fifty-microliter aliquots were removed at specific times and added to 100 ml of quench buffer (Buffer G + 10 mM $MgCl_2$, 100 mM GTPγS, 100 mM timolol) on ice. Samples were filtered on GF/B 96-well plates as above, except that filters were washed five times with ice-cold 20 mM Tris-HCl pH 8, 100 mM NaCl, 10 mM $MgCl_2$. The glass-fiber filtration method was selected over the more traditional nitrocellulose filter method (including detergent, Lubrol) to be consistent with the conditions selected for the radioligand-binding assays. In addition, to avoid disrupting the rHDL particles, we excluded detergent (Lubrol) from our binding and filtration steps, the inclusion of which could enhance the recovery of [^{35}S]GTPγS binding to G proteins on nitrocellulose filters by as much as 50%.

To quantitate total G protein in the reconstitution capable of binding [^{35}S]GTPγS, we did, however, use more traditional methods. Total [^{35}S]GTPγS binding was assessed in Buffer H plus 50 mM MgCl2, 10 mM [^{35}S]GTPγS, 0.05% Lubrol. After incubating for 30 min at 30°C, samples were rapidly filtered through BA-85 nitrocellulose filters (Whatman) and washed 4 x 2 ml with ice-cold 20 mM Tris-HCl pH 8, 100 mM NaCl, 10 mM $MgCl_2$. Using nitrocellulose filtration and inclusion of detergent (Lubrol) to determine the total [^{35}S]GTPγS binding to G protein, we obtain data that are consistent with our observations using glass-fiber filtration. Our data suggest that 20% of the [^{35}S]GTPγS-binding activity survives the reconstitution step, only a portion of which (29 +/- 5% of the 20% [^{35}S]GTPγS binding, or 5.8% of the G protein added to the reconstitution) copurifies with the β_2AR•rHDL on an anti-FLAG resin (the β_2AR is FLAG-tagged). No binding was observed in the column flowthrough or wash fractions.

Thus, the remaining two-thirds appears to remain on the anti-FLAG column, presumably in the form of an aggregate that is capable of binding [^{35}S]GTPγS. The remaining 14% of the total G protein will be present in the assay, but as an aggregate and unlikely to be accessible to the β_2AR in rHDL.

On the surface, the presence of the aggregates that are capable of binding [^{35}S]GTPγS could confound the results and interpretation of the data in ***Fig. 2-7a***. However, the conditions used in ***Fig. 2-7a*** (100 nM [^{35}S]GTPγS, 2 mM $MgCl_2$) are dramatically different from those used to measure total [^{35}S]GTPγS binding (10 mM [^{35}S]GTPγS and 50 mM MgCl2). Such conditions of low nucleotide concentrations, such as those used in ***Fig. 2-7a***, should display a preference for detection of receptor-stimulated G protein binding.

Cross-linking of Cy3-β_2AR. The bifunctional amine-reactive cross-linkers *bis*(sulfosuccinimidyl) suberate (BS^3, 11.4 Å spacer arm) or *bis N*-succinimidyl[pentaethylene glycol] ester (*Bis*(NHS)PEO_5, 21.7-Å spacer arm) were purchased from Pierce Biotechnology (Rockford, IL). BS^3 stock solutions of 100 mM were prepared from solid reagent in Buffer H + 0.1% DDM or dimethyl sulfoxide immediately before each use. Cross-linking reactions of Cy3-β_2AR in detergent micelles were performed in Buffer H plus 0.1% DDM at a final receptor concentration of 2 μM. Cross-linking reactions of Cy3-β_2AR reconstituted in lipid vesicles were performed in Buffer H at a final receptor concentration of ≈250 nM. The final concentrations of either *Bis*(NHS)PEO 5 or BS^3 used in each case were 0, 0.25, 0.5, 1.0, 2.5, and 5.0 mM. After addition of cross-linker stock solution, the samples were mixed by inverting and incubated for 2 h on ice. The reaction was quenched by addition of 20 mM Tris. The

cross-linked samples were then analyzed by SDS-PAGE (10% gels) with ≈0.5 μg of protein loaded in each well. Cy3 fluorescence was directly visualized using a FluorChem 8800 (Alpha Innotech) imaging system.

Photobleach step analysis. To assess the labeling stoichiometry of fluorescent receptors, the number of photobleaching steps was counted manually from the time traces of at least 400 molecules of each Cy3-β_2AR, Cy5-β_2AR, Cy3-β_2AR•rHDL, and Cy5-β_2AR•rHDL. The number of photobleaching steps represents the number of detectable fluorophores bound to a receptor at the time of imaging. Receptors were classified as being single-, double-, or triple-labeled based on the observed number of photobleaching steps. In some cases, the precise number of photobleaching steps could not be discerned from the time trace (usually due to low signal-to-noise or fluorophore blinking). Such molecules were classified as "not countable". We used the most conservative estimate of the labeling efficiency, by assuming that all molecules in the "not countable" category are actually single-labeled.

To estimate the fraction of unlabeled receptor in each sample, we simulated the labeling kinetics of the three most reactive cysteines of the β_2AR using a mathematical model. For WT β_2AR, cysteine-265 is ≈10 times more reactive than the next most reactive cysteine. Given the reactivity of cysteine-265, it is intuitive that the vast majority of receptors should become singly-labeled before an appreciable fraction becomes multiply-labeled. The model confirmed this suspicion, and was able to accurately reproduce the observed fractions of double-and triple-labeling with fluorophore. The model consists of the following reactions that are equally valid for Cy3 or Cy5.

1. $\beta_2AR + Cy3 \xrightarrow{k_{Cys265}} Cy3\text{-}\beta_2AR$
2. $Cy3\text{-}\beta_2AR + Cy3 \xrightarrow{k_2} (Cy3)_2\text{-}\beta_2AR$
3. $(Cy3)_2\text{-}\beta_2AR + Cy3 \xrightarrow{k_2} (Cy3)_3\text{-}\beta_2AR$

The model is described by a set of coupled differential equations:

$$\frac{d[\beta_2AR]}{dt} = -k_{Cys265}[\beta_2AR][Cy3]$$
$$\frac{d[Cy3\text{-}\beta_2AR]}{dt} = k_{Cys265}[\beta_2AR][Cy3] - k_2[Cy3\text{-}\beta_2AR][Cy3]$$
$$\frac{d[(Cy3)_2\text{-}\beta_2AR]}{dt} = k_2[Cy3\text{-}\beta_2AR][Cy3] - k_2[(Cy3)_2\text{-}\beta_2AR][Cy3]$$
$$\frac{d[(Cy3)_3\text{-}\beta_2AR]}{dt} = k_2[(Cy3)_2\text{-}\beta_2AR][Cy3]$$
$$\frac{d[Cy3]}{dt} = -k_{Cys265}[Cy3][\beta_2AR] - k_2[Cy3]([Cy3\text{-}\beta_2AR] + [(Cy3)_2\text{-}\beta_2AR])$$

[**1**]

We assumed that each reaction is irreversible and that only cysteine-265 can react with the first fluorophore (Eq. **1**). The equations were solved numerically with Mathematica (Wolfram Research, Inc., Champaign, IL) using the following parameters: *k*Cys-265 = 0.8 s^{-1} μM^{-1}, k2 = 0.08 s^{-1} μM^{-1}, initial [β_2AR] = 5 μM. The rate constants are based on the reactivity of WT and C265A β_2AR as measured by fluorescein maleimide labeling as previously described [86]. The total concentration of Cy3 incorporated was arbitrarily chosen as 7.2 μM, because this value accurately reproduces the fractions of single-, double-and triple-labeling as measured by photobleach step counting (model results 64% single-labeled, 28% double-labeled, 8% triple-labeled, and 0.4% unlabeled at steady-state,

assuming all "not countable" molecules are actually singly-labeled). This [Cy3] corresponds to a labeling efficiency of 1.4 mol fluorophore per mol of β2AR, in good agreement with our absorbance measurements (1.6-2.5 fluorophores per protein; see text).

CHAPTER 3

EFFICIENT COUPLING OF TRANSDUCIN TO MONOMERIC RHODOPSIN IN A PHOSPHOLIPID BILAYER

Introduction

G protein-coupled receptors (GPCRs) are an important class of cell surface receptors representing the third largest gene family in the human genome [87]. They recognize a wide variety of extracellular stimuli (e.g. light, tastes, odors, hormones, neurotransmitters, and cytokines, etc.) leading to direct activation of intracellular and membrane-associated G proteins, that in turn regulate various downstream effectors (e.g. adenylyl cyclase, phospholipase C_β and ion channels, etc.) [2]. This diversity highlights nature's ability to generate specificity in signal detection and propagation and thus make GPCRs optimal therapeutic targets.

To complicate the pharmacology of these targets, GPCRs associate as oligomers of two or more receptors in cellular membranes [88]. The growing list of GPCRs that form either hetero- or homomeric complexes implies that oligomerization is important. However, an essential role of oligomerization for GPCR family function has not been established.

Evidence that an isolated, monomeric GPCR in a biological membrane is fully capable of stimulating nucleotide exchange by G proteins has been difficult to

demonstrate. Intuitively, detergent solubilization and monodispersion of membrane proteins into micelles should represent a suitable substitute for a phospholipid bilayer. However, mounting evidence suggests otherwise, as detergents can have profound deleterious effects on the structure and function of membrane proteins [37-39].

Here we employ high density lipoprotein (HDL), a nanometer-scale apolipoprotein A-I (apoA-I)-wrapped phospholipid bilayer that is naturally involved in the reverse cholesterol transport pathway [48], to reconstitute the photoreceptor GPCR, rhodopsin (Fig. 1). A similar membrane protein reconstitution system has been developed by the Sligar laboratory for numerous proteins including the proton pump bacteriorhodopsin [47], cytochrome P-450 [46], the β_2-adrenergic receptor [89] and, more recently, rhodopsin [90]. The HDL platform represents a dramatic improvement over detergent micelles for maintaining GPCRs in a monomeric and monodispersed state.

Here we report the isolation of bovine rhodopsin, a prototypical GPCR [9, 91], in reconstituted HDL (rHDL) particles (***Fig. 3-1***). We take advantage of the unique spectral qualities of rhodopsin to demonstrate that it exists as a monomer in rHDL and to follow its activity and behavior compared to rhodopsin in native membranes isolated from rod outer segments (ROS). We find that the rates of formation and decay of metarhodopsin II (Meta II), the active form of the receptor, for monomeric rhodopsin are identical to those observed in ROS. We also show that monomeric rhodopsin is capable of stimulating rapid nucleotide exchange on G_t transducin, a photoreceptor-specific G protein at rates comparable to those observed in ROS. These data show that monomeric rhodopsin is fully functional with regard to G protein activation and suggest that receptor oligomerization does not play an essential role in this process.

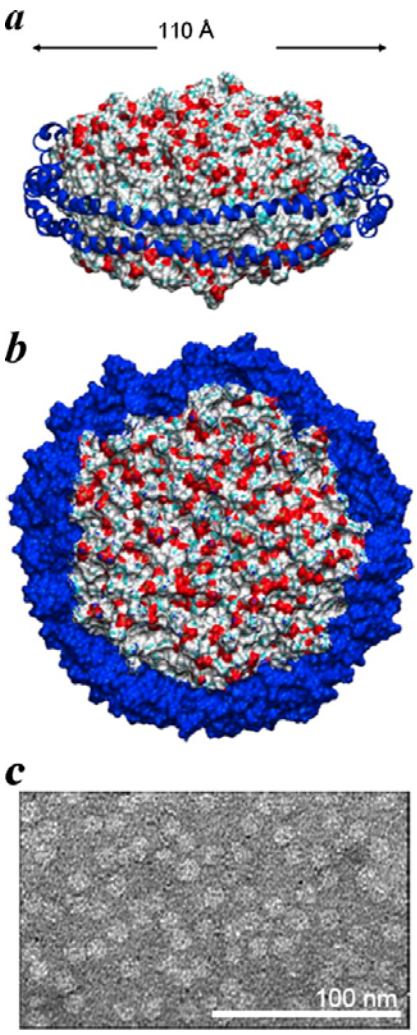

Figure 3-1. Illustration of reconstituted HDL particles. ***a*** and ***b***, molecular models illustrating a dimer of apoA-I proteins wrapped around a phospholipid bilayer consisting of 160 POPC molecules. Each apoA-I protein (*blue*) is depicted as a ribbon diagram. ***c***, electron micrograph of rHDL particles reveal monodisperse and homogeneous rHDL particles. Images in ***a*** and ***b*** were produced using PyMol (DeLano Scientific LLC, Palo Alto, CA). Coordinates for the HDL model from Segrest *et al.* [70] were obtained on line and used with permission from Dr. Stephen Harvey.

Results

Reconstitution of rhodopsin in HDL. Photoactivation of rhodopsin results in the isomerization of its covalently-bound ligand 11-*cis*-retinal (absorbance maximum, λ=500 nm) to all-*trans*-retinal, creating Meta II (λ=380 nm), a spectroscopically distinct

form [8]. Because rhodopsin requires a particular lipid environment (lipids that have 16 carbons or greater and are unsaturated) in order to transition to the active Meta II state [92], a mixture of POPC:POPG (3:2) was utilized for the lipid component of the rHDL. POPC alone was also used successfully (data not shown).

Incorporation of rhodopsin into rHDL, in the presence of excess rHDL yielded particles with Stokes diameters of 10.5 nm based on detection at λ=280 nm as assessed by size exclusion chromatography (SEC) whereas the peak at absorbance at λ=500 nm eluted with an estimated diameter of 11 nm (***Fig. 3-2a***). Analysis of the peak SEC fraction by spectroscopy indicates that rhodopsin in rHDL is functional as it photoisomerized to the active Meta II state (***Fig. 3-2b***).

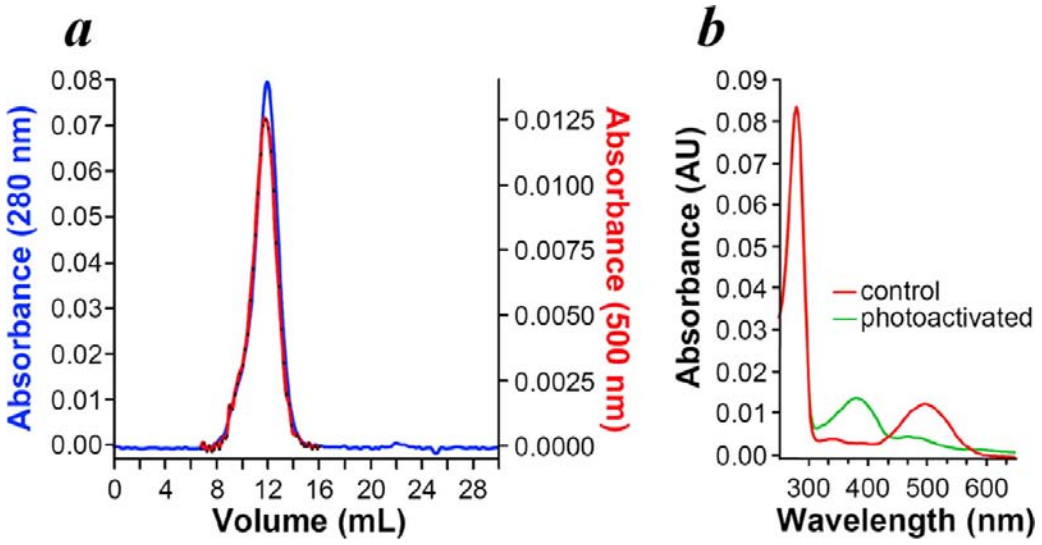

Figure 3-2. Rhodopsin incorporated in rHDL and resolved by size exclusion chromatography is photoactivatable. **a**, purified bovine rhodopsin incorporated into rHDL particles was resolved on a Superdex 200 size exclusion column; fractions (200 µl) were collected and analyzed for λ = 280 nm (blue) and λ = 500 nm (red) absorbance. **b**, peak fraction from the gel filtration run was adjusted to pH 6.5, and UV-visible spectra were measured before and after photoactivation.

It is important to note that removal of the detergent in the absence of lipid and/or apoA-I, severely alters the integrity of rhodopsin. If either component is excluded, most of the rhodopsin precipitates and pellets after a brief sedimentation (16,000*g* for 2 min) in a microcentrifuge. Any rhodopsin that seemed not to sediment migrated in the void volume of the size exclusion column, suggesting that it formed large protein aggregates or was contained in proteoliposomes (data not shown). When both components were included, we routinely observed reconstitution efficiencies of 70-90%, based on absorbance at λ=500 nm.

Fraction	A_{280}	A_{500}	[Rhodopsin]:[apoAI]
ConA-Sepharose column			
Load	1	0.15	0.15
Flow-through	0.57	0.02	0.035
Elute 2	0.12	0.04	0.47
Elute 3	0.07	0.02	0.47
Elute 4	0.04	0.01	0.42
SEC column			
Load			0.46
SEC average			0.47 ± 0.05

Figure 3-3. Rhodopsin·rHDL particles were resolved on a size exclusion column and then purified on a ConA-Sepharose column. The load, flow-through, and three serial elutions from the ConA-Sepharose column were assayed for absorbance at λ = 280 nm and λ = 500 nm. ConA-Sepharose column eluates were pooled and re-resolved on a size exclusion column in order to confirm that the size of the rhodopsin·rHDL particles remained the same before and after processing by the ConA-Sepharose column. The average A280:A500 ratios of all fractions across the peak were calculated as described under "Experimental Procedures."

Rhodopsin:rHDL stoichiometry. To determine the rhodopsin:rHDL stoichiometry, we utilized the known extinction coefficients for both, rhodopsin (at

λ=280 and λ=500 nm) and apoA-I (at λ=280 nm), to calculate the molar ratio of [rhodopsin]:[apoA-I] in purified rhodopsin•rHDL preparations. Rhodopsin•rHDL was purified by either Con A Sepharose (taking advantage of the glycosylated rhodopsin) (***Fig. 3-3***) or by immunoaffinity chromatography (1D4 antibody against rhodopsin) (data not shown) and then resolved by SEC (***Fig. 3-4a***).

The average [rhodopsin]:[apoA-I] molar ratio of the SEC peak fractions was determined to be 0.47 ± 0.05 (***Fig. 3-3*** and ***Fig. 3-4a***). Taking into consideration that there are two apoA-I proteins per rHDL particle [50, 93], these data suggest that only one rhodopsin molecule is reconstituted per rHDL. The purified rhodopsin•rHDL complexes also had a Stokes diameter of 11 nm based on their elution volume from the SEC column (***Fig. 3-4a***). This rules out the possibility that larger rHDL particles were formed (i.e. 2 rhodopsins to 4 molecules of apoA-I, still in a 0.5:1 ratio). Moreover, TEM of the 1D4-immunopurified rhodopsin•rHDL complexes shows a monodisperse and homogeneous rhodopsin•rHDL particle morphology with an estimated diameter of 13.7 +/- 1.4 nm (n=105, ***Fig. 3-b***). We attribute the slightly larger diameter compared with those estimated by SEC and the previously reported HDL sizes [94] to a commonly observed flattening artifact of particles by surface tension during drying of the stain [95, 96]. Atomic force microscopy confirms that these particles are discoidal with a thickness of about 43 +/- 4.7 Å, similar to that of a single phospholipid bilayer [97] (data not shown).

Functional comparison of monomeric and oligomeric rhodopsin. To assess the function of rhodopsin incorporated into rHDL, we performed UV/Vis absorbance scans of these reconstitutions before and after photoactivation (***Fig. 3-5a***). Exposure to light resulted in a rapid and almost complete conversion of the absorbance spectra of

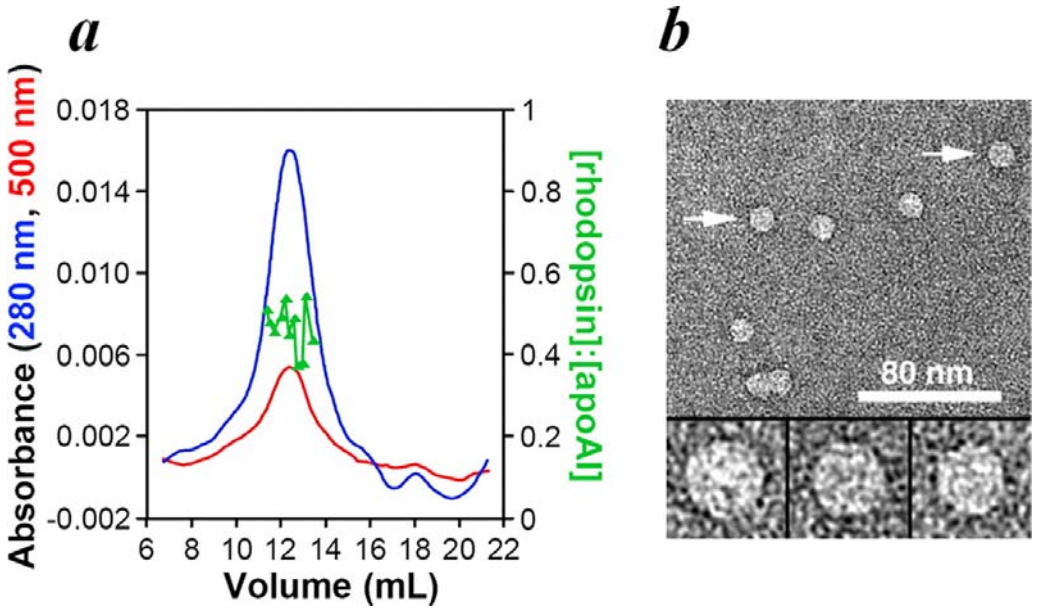

Figure 3-4. Rhodopsin exists as a monomer in rHDL particles. **a**, rhodopsin incorporated into rHDL particles was purified on a ConA-Sepharose column and subsequently resolved on a size exclusion column. Eluates were assayed for absorbance at λ = 280 nm (blue) and λ = 500 nm (red), and the rhodopsin: apoA-I ratio (green) was calculated as described under "Experimental Procedures." **b**, TEM of negatively stained purified rhodopsin·rHDL particles showing their homogeneous discoidal shapes and monodispersed distribution.

rhodopsin•rHDL from λ=500 nm (rhodopsin) to λ=380 nm (Meta II). Over a time course of 30 min, Meta II slowly decayed to both free all-*trans*-retinal (as observed in the slight red-shift of the λ=380 nm peak) and Meta III (as observed in the increase of the λ=465 nm peak). This sequence is identical to that observed for rhodopsin in native ROS membranes [8] as well as for rhodopsin reconstituted in long-chain, unsaturated lipid vesicles [92, 98]. Using the method of Farrens and Khorana [99], we determined that the time constant, τ, for the Meta II decay for rhodopsin in rHDL was 19.2 +/- 0.8 min (***Fig. 3-5c***), nearly identical to the decay rate of rhodopsin from ROS (20 +/- 2.4 min) (***Fig. 3-5b)*** and similar to previously observed values [100].

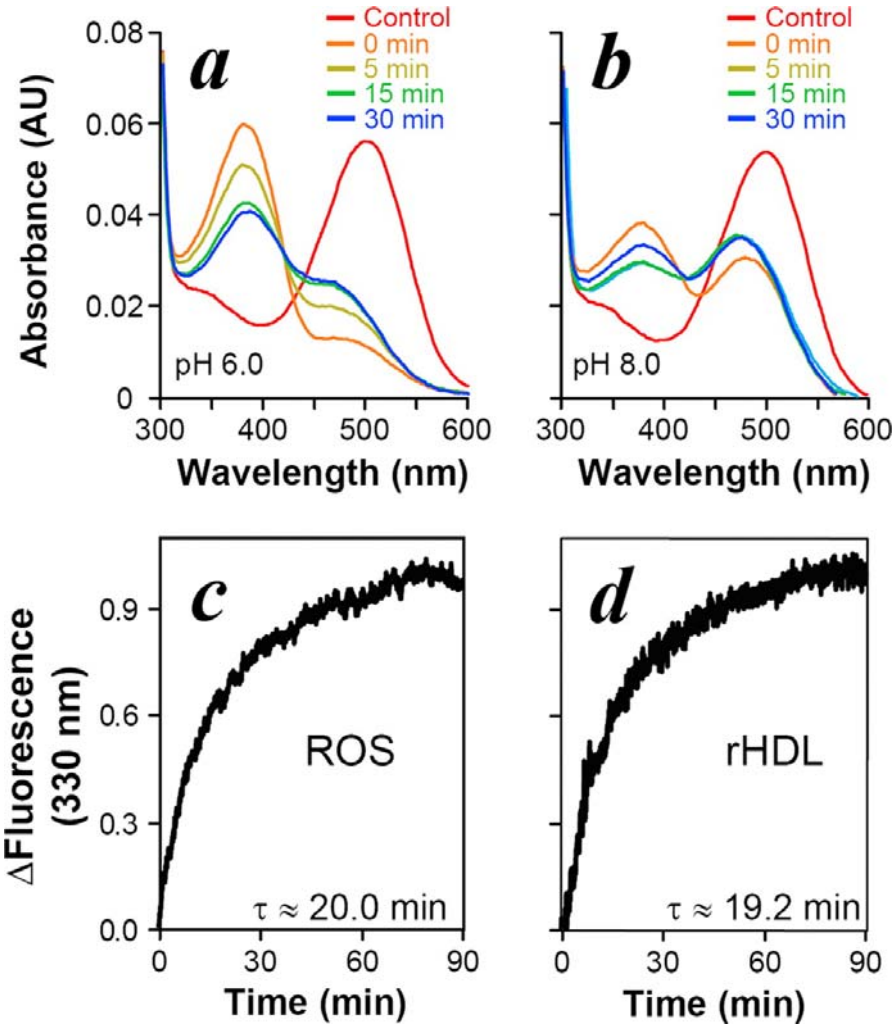

Figure 3-5. Meta II formation and decay. UV-visible spectra were measured from a rhodopsin·rHDL preparation before (red), and at 0 (orange), 5 (olive), 15 (green), and 30 min (blue) after photoactivation at pH 6.5 (**a**) or pH 8.0 (**b**). The rate of meta II decay was measured by exciting 10 nM rhodopsin in ROS membranes (**c**) or rHDL (Rho·rHDL) (**d**) at λ = 295 nm and measuring emission at λ = 330 nm emission following a 15-s photoactivation using the methods of Farrens and Khorana (20). The relaxation times (τ) shown were calculated from three independent experiments.

Unlike other members of the heterotrimeric G protein family, transducin (G_t) can be suspended in solution in the absence of detergent [101]. Transducin activation may be accomplished by simply adding the heterotrimer to rhodopsin preparations, whether in ROS membranes or as a purified protein. ***Figure 3-6a*** illustrates that activation of transducin by photoactivated rhodopsin from ROS membranes, at 9:1 G_t:rhodopsin ratio,

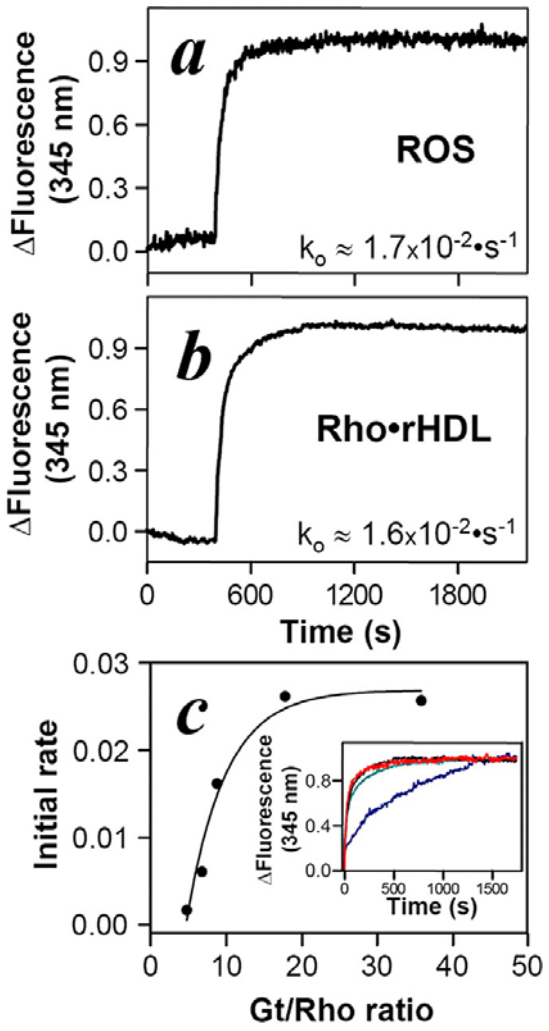

Figure 3-6. Activation of transducin by monomeric rhodopsin in rHDL. Photoactivated oligomeric rhodopsin in ROS membranes (**a**) or monomeric rhodopsin in rHDL (**b**) activates transducin at identical rates. Transducin was added to pre-activated photoactivated rhodopsin in rHDL or in ROS membranes at a 9:1 ratio as described under "Experimental Procedures." Transducin activation was measured by monitoring the tryptophan fluorescence (λ_{em} = 345 nm) of the Gtα subunit. Initial rates based on the least squares fit of the data to an exponential activation are illustrated in the lower corner of each panel and were calculated from three independent experiments. **c**, elevating the Gt:rhodopsin ratio increased the rate of Gt activation (initial rate, s^{-1}) in rhodopsin·rHDL particles (Rho·rHDL). The effect of increasing Gt:rhodopsin ratios appears to be a titration of the observed rates. The maximal rate was achieved at a Gt:rhodopsin ratio of 12:1.

occurred with a rate constant of approximately 1.7×10^{-2} s^{-1}, comparable to previously reported values [100, 102]. Strikingly however, activation of monomeric rhodopsin in

rHDL occurred at an identical rate (***Fig. 3-6b***). These data differ markedly from previously reported rates of activation of transducin by detergent-solubilized rhodopsin in different oligomeric states where rhodopsin oligomers were 3 times faster than monomers in activating transducin [103]. Titration with increasing G_t: rhodopsin•rHDL ratios raised the rate of activation to a maximal rate of approximately 2.6×10^{-2} s^{-1} (***Fig. 3-6c***). Maximal rates were obtained at G_t: rhodopsin•rHDL ratios of approximately 12:1.

Discussion

Receptor oligomerization has become the subject of considerable attention in the GPCR field. A plethora of studies using elegant approaches have provided descriptive evidence of receptor homo- and/or heterodimerization of visual receptors and many hormone receptors [58, 104]. Comparatively fewer contributions, however, have provided evidence for functional roles of oligomerization. Targeting roles of receptor hetero-oligomers have been suggested for the $GABA_{B1}$ and $GABA_{B2}$ receptors [97, 105] or with the α_{1B}- and α_{1D}-adrenergic receptors [32]. Biophysical and biochemical approaches have also suggested receptor-receptor cooperativity of homo-oligomers of the metabotropic glutamate receptors [80] or leukotriene B4 receptors [34]. In addition, a growing body of evidence suggests that most GPCRs exist as oligomers in cellular membranes, complexes that are found in the endoplasmic reticulum and Golgi apparatus and thus occur during receptor maturation (reviewed by Bulenger *et al*. [106]). Previously reported imaging data of native retinal disc membranes also suggest that certain receptor types, such as rhodopsin, are capable of organizing into higher-order oligomers [10, 107].

However, the question as to whether G protein activation is dependent on oligomerization has yet to be elucidated.

Data presented here suggest that a monomeric GPCR is as effective as an oligomeric receptor in activating a G protein. Transducin activation by rhodopsin in rHDL behaves in a manner that is kinetically indistinguishable from that of oligomeric rhodopsin found in ROS membranes. Moreover, the monomeric rhodopsin data are consistent with early studies addressing single photon responses of rod cells, demonstrating that one activated rhodopsin per cell triggers phototransduction [108]. Our ability to observe faster rates of transducin activation by monomeric rhodopsin in rHDL particles compared to rhodopsin in detergent likely reflects the combined effects of lipids on rhodopsin structure and on G protein incorporation. The heterotrimeric G protein transducin is lipid-modified on both the amino-terminus of $G_t\alpha$ (myristoylation) and the carboxy-terminus of $G\gamma_1$ (isoprenylation) subunits and both these modifications have been shown to contribute to G protein interaction with rhodopsin [3, 4]. Although many studies suggest that monomeric rhodopsin in detergent micelles represents the minimal functional unit (reviewed in [57]), few of them report the isolation and characterization of monomeric rhodopsin in a membrane environment. Reconstitution of monomeric rhodopsin into a phospholipid bilayer such as rHDL therefore represents a significant advance in our understanding of the contributions of homo-oligomerization of this photoreceptor and perhaps most GPCRs. A recent report by Bayburt *et al.* used a similar approach to incorporate both monomers and dimers of rhodopsin in rHDL-like particles termed nanodiscs [90]. In that study, however, the dimeric form was found to be only half as effective in activating transducin as the monomeric form but it still operated at rates

considerably faster than those observed in detergent micelles. Such data apparently contrast to our findings with native ROS membranes where the rates of transducin activation of monomeric and oligomeric forms are identical. A plausible explanation is the possibility that "antiparallel" dimers (i.e., N-termini located on opposite sides of the phospholipid bilayer) may have incorporated into the nanodiscs. Transducin coupling to antiparallel dimers may not be optimal under these conditions.

Our monomeric G_t•rhodopsin•rHDL data strongly suggest that whereas oligomerization occurs with rhodopsin, and perhaps most GPCRs, the minimal G protein signaling unit is likely a monomer. Our data contradict a previously suggested interpretation that rates of activation of transducin depend on rhodopsin oligomeric states [103]. The simplest explanation for this discrepancy could be that the presence of phospholipids surrounding a rhodopsin molecule is critical for efficient precoupling and fast G_t activation. The model of the rhodopsin monomer as a G protein signaling unit is still consistent with the implication that the smallest organized unit, a homodimer, may contain only one photoreceptor that participates in G protein activation (illustrated in ***Fig. 3-7***). Such a pentameric, rhodopsin-G protein complex was previously proposed by Filipek and colleagues [35], a model that has also been proposed for the $GABA_B$ receptor [78, 109], mGlu receptor [80], LtB4 receptor [67] and α_{1B}/α_{1D} adrenergic receptor [32].

In summary, our data show that a reconstituted monomeric GPCR is capable of activating a G protein as efficiently as its native receptor oligomer. Similar rates of transducin activation by rhodopsin•rHDL compared to ROS membranes suggest that oligomerization is not essential for G protein activation. Rather, GPCR oligomerization may contribute toward fine tuning of photoreceptor responses, receptor stabilization,

targeting and desensitization. Indeed, the 'double chalice' structure of arrestins infers that its interaction may be significantly enhanced by receptor oligomerization [110-112]. The recruitment of arrestin to GPCRs and therefore the recruitment of various kinases (e.g.,

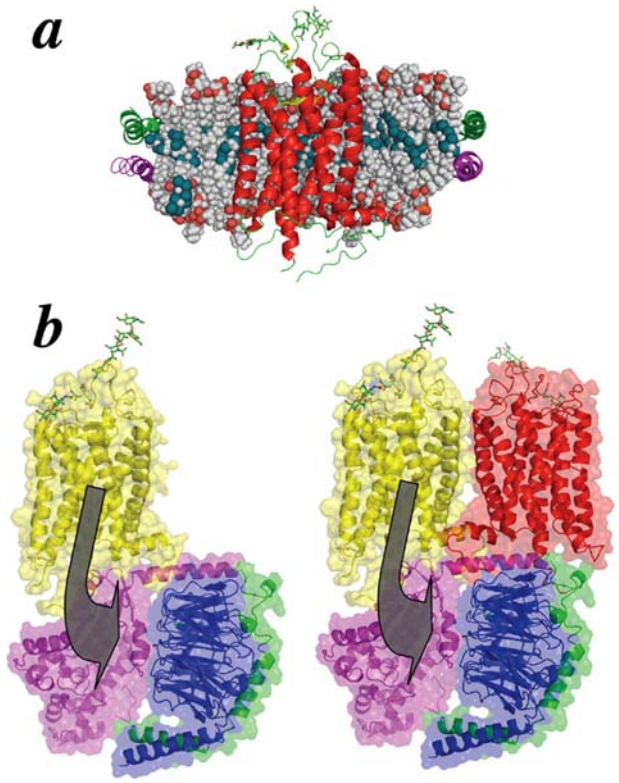

Figure 3-7. Only one receptor in a receptor dimer is necessary to activate G proteins. **a**, molecular model of a rhodopsin monomer in a rHDL (cross-section, side view). **b**, model illustrating monomeric rhodopsin in comparison to oligomeric (dimeric) rhodopsin coupling to a single G protein heterotrimer. The activated form of rhodopsin (meta II, yellow) in a dimeric form with rhodopsin (red) in a complex with transducin: Gtα (magenta), Gβ1 (blue), and Gγ1 (green). The coordinates for rhodopsin[71] and transducin[113] were obtained from the RCSB Protein Data Bank, accession number 1F88 and 1GOT, respectively. The conceptual model of a dimeric rhodopsin, where one molecule is activated, with a single Gt was previously proposed by Filipek *et al.*[35].

Src, Raf and ERK) has been proposed to serve as an important, non-G protein-dependent function of the superfamily of seven-transmembrane spanning receptors [114]. Future studies will undoubtedly reveal the underlying functions of oligomerization itself and the contributions it makes toward recruitment of important signaling partners.

Materials and Methods

Materials. Expired human sera were generously donated by Dr. Bert La Du (University of Michigan). All lipids were purchased from Avanti Polar Lipids (Alabster, AL). N-dodecyl-β-D-maltoside (DDM) was obtained from Dojindo Molecular Technologies (Gaithersburg, MD). Triton X-100 and sodium cholate were purchased from Sigma-Aldrich (St. Louise, MO). Frozen bovine retina were obtained from J. A. Lawson Co. (Lincoln, NE). All other reagents were of analytical grade.

Purification of human apoA-I. ApoA-I was purified from human serum essentially as described by Gan *et al.* [82]. Briefly, clarified serum was diluted into a conditioning buffer: 50 mM Tris-HCl, pH 8.0, 1 mM $CaCl_2$, 3 M NaCl, 5 mM EDTA and added to an equal volume of Cibacron blue F3GA-agarose (Sigma-Aldrich) equilibrated in 50 mM Tris-HCl, pH 8.0, 1 mM $CaCl_2$, 3 M NaCl, 5 mM EDTA (Buffer A). The slurry was stirred for 30 min and then batch washed by filtration through a Whatman #1 filter in a Büchner funnel five times with Buffer A or until the absorbance (λ=280 nm) of the filtrate was less than 0.025 OD The resin was then washed with two additional volumes of Buffer A without NaCl (Buffer B). The residual cake was resuspended in an equal volume of Buffer B and transferred to a column. ApoA-I was then eluted with Buffer B containing 5 mM cholate, yielding fractions with purities typically between 80-90 %. Peak fractions were pooled, concentrated and then diluted 1:1 in 25 mM Tris-HCl, pH 8.0, 1 mM $CaCl_2$, 5 mM EDTA, 0.2 % Triton X-100 and loaded on to a Q Sepharose (GE Healthcare, Piscataway, NJ) column. The column was washed with 20 mM Tris-HCl, pH 8.0, 1 mM $CaCl_2$, 5 mM EDTA, 0.1 % Triton X-100 (Buffer C) and eluted with a shallow linear gradient with Buffer C, containing 1 M NaCl. Peak fractions (> 95 %

purity) were buffer exchanged into 100 mM K-acetate pH 5.0, 1 mM EDTA, 0.1 % Triton X-100 and applied to a SP Sepharose (GE Healthcare) column equilibrated in 25 mM K-acetate pH 5.0, 1 mM EDTA, 0.1 % Triton X-100 (Buffer D). The column was washed in Buffer D and apoA-I was eluted with a linear gradient of Buffer D containing 1 M NaCl. Residual contaminants were removed by size exclusion chromatography on a Superdex 200 column (GE Healthcare) in 20 mM Hepes-NaOH, pH 8.0, containing 100 mM NaCl, 1 mM EDTA, 20 mM cholate, at 4 °C. ApoA-I fractions were pooled and concentrated (~10 mg/mL), then dialyzed at 4 °C against 20 mM Hepes-NaOH, pH 8.0, 100 mM NaCl, 1 mM EDTA, 5 mM cholate and stored at –80 °C until further use.

Purification of bovine rhodopsin. Rhodopsin was purified from ROS isolated from bovine eyes as previously described [115], a procedure that yielded rhodopsin with a $A_{280\ nm}/A_{500\ nm}$ absorbance ratio of 1.63. $ZnSO_4$ was removed by dialysis in the presence of 0.1% DDM (final) to avoid precipitation of added cholate during the subsequent rHDL preparation.

In vitro reconstitution of HDL. HDL was reconstituted *in vitro* essentially as described by Jonas [50] with slight modifications. Palmitoyl-oleoyl-phosphatidylcholine (POPC), and palmitoyl-oleoyl-phosphatidylglycerol (POPG) were used in combination at a 3:2 molar ratio to mimic the zwitterionic environment of a cell membrane [40]. Lipids were dried under argon (or nitrogen) from a chloroform solution and desiccated for 30-60 min to remove residual chloroform. Then briefly, lipids were solubilized in 20 mM Hepes-NaOH, pH 8.0, 100 mM NaCl, 1 mM EDTA (Buffer A) containing 50 mM detergent (DDM or cholate) and added to purified rhodopsin. ApoA-I then was added and the mixture incubated for 1-2 hr on ice. The final concentrations of the components were

1 μM rhodopsin, 24 mM detergent, 8 mM lipids, and 100 μM apoA-I. This mixture was added to BioBeads (BioRad, Hercules, CA) to remove detergents. Samples were stored on ice until used. All of the above procedures were performed under dim red light $\lambda >$ 640 nm.

Analytical size exclusion chromatography. Analytical size exclusion chromatography was performed on a HR10/30 column (GE Healthcare) packed with about 20 mL Superdex 200 preparative resin (GE Healthcare) (Vo = 7 mL). The column was calibrated with thyroglobulin (molecular weight (MW) 669 kDa, Stokes diameter (Sd) 17.2 nm, elution volume (Ve) 9.1 mL, apoferritin (MW 432 kDa, Sd 12.2 nm, Ve 10.6 mL), alcohol dehydrogenase (MW 150 kDa, Sd 9.1 nm, Ve 13.2 mL), bovine serum albumin (MW 66 kDa, Sd 7.2 nm, Ve 14.7 mL), and carbonic anhydrase (MW 29 kDa, Sd 4 nm, Ve 17.8 mL). Samples were loaded in 100-500 μL static loops and run at a flow rate of 0.7 mL/min using the BioLogic DuoFlow system (BioRad) at 4 °C. Column fractions, 200 μL each, were collected in a 96-well plate for further analysis. Chromatography of rhodopsin samples was performed under dim red light.

UV/Vis absorbance assays. All UV/Vis absorbance assays were performed in UV-transparent 96-well plates (Corning, Lowell, MA) on a SpectraMax 190 plate reader (Molecular Devices, Sunnyvale, CA). The PathCheck™ feature was used for normalizing path lengths to 1 cm. Rhodopsin concentrations were determined by the absorbance change at λ=500 nm before and after bleaching. A value of 40,600 M^{-1} cm^{-1} used as the extinction coefficient [116]. Rhodopsin photoactivation was achieved by illuminating samples for 15 s with a 500 W halogen lamp affixed with a 495 nm long-pass filter (Melles Griot, Rochester, NY).

Meta II formation and decay spectra. Rhodopsin samples were adjusted to pH 6.5 and photoactivated as described above. Subsequent absorbance spectra were recorded at 0, 5, 10, 15 and 30 min. Meta II decay rate determinations were performed by the Trp fluorescence (λ_{ex}=295 nm and λ_{em}=330 nm) method of Farrens and Khorana [99]. All measurements were performed with 10 nM rhodopsin dissolved in buffer consisting of 10 mM Bis-Tris-HCl, pH 6.0, containing 100 mM NaCl, which favors the formation of Meta II, the activated, signaling form of rhodopsin. A Perkin Elmer LS 55 Luminescence Spectrophotometer was used to measure the intrinsic fluorescence increase due to Trp residues that correlates with the decrease in the protonated Schiff base concentration (data not shown but consistent with Refs. [99, 102, 117]). Rhodopsin•rHDL or ROS membranes were bleached by a Fiber-Lite illuminator for 15 s immediately before the fluorescence measurements. Bleaching was carried out from a distance of 15 cm, to prevent heat accumulation and a thermostat was applied to stabilize the temperature of the cuvette at 20ºC. Fluorometer slit settings were 2.5 nm at λ=295 nm for excitation and 8.0 nm at λ=330 nm for emission.

Rhodopsin:ApoA-I molar ratio. Rhodopsin:ApoA-I ratios were determined from Concanavalin A (ConA)-Sepharose [118] or immunoaffinity (monoclonal 1D4) [119] chromatography-purified rhodopsin•rHDL using the known extinction coefficients for rhodopsin (40,600 $M^{-1}cm^{-1}$ at λ=500 nm) [116] and apoA-I (31,720 $M^{-1}cm^{-1}$ at λ=280 nm) [120] and the known 280 nm to 500 nm absorbance ratio of pure rhodopsin of 1.6. The rhodopsin concentration was calculated as: [rho] = A_{500} / 40,600. The apoA-I concentration was calculated as: [apoAI] = A_{280} (due to apoA-I only) / 31,720, where A_{280} (due to apoA-I only) = A_{280} (total) – A_{280} (due to rhodopsin only), and A_{280} (due to

rhodopsin only) = A_{500} x 1.6.

Activation of transducin. Photoactivation of G_t was performed as previously described [100, 121]. Gt concentrations were determined by a Bradford assay (BioRad). Purified, native bovine G_t heterotrimer ($G_t\alpha,\beta_1,\gamma_1$) was added to rhodopsin in bovine ROS membranes that were sonicated before measurement, or to rhodopsin•rHDL, at a G_t:rhodopsin ratio of 9:1 at a concentration of 250 nM and rhodopsin at 30 nM (within the linear range of fluorescence change and protein concentration). The measurement of intrinsic Gt fluorescence at 345 nm was performed in a buffer consisting of 20 mM Bis-Tri-HCl, pH 6.0, containing 120 mM NaCl and 6 mM $MgCl_2$. The sample was bleached for 15 s with a Fiber-Lite covered by a long-pass wavelength filter (λ >490 nm) and followed by a 400 sec incubation with continuous low-speed stirring. Then GTPγS was added and the intrinsic fluorescence increase from Gt was measured with a Perkin Elmer LS 55 Luminescence Spectrophotometer. No signals from rhodopsin were detected in control experiments without transducin (not shown).

Transmission Electron Microscopy (TEM). Reconstituted HDL samples were placed on a carbon-coated copper grid and stained with 1 % phosphotungstic acid, pH 6.5. Samples were imaged with a Philips CM-100 transmission EM operating at 60 kV. Purified (either ConA or 1D4-immunoaffinity) rhodopsin•rHDL particles were adsorbed for 10 s to parlodion carbon-coated copper grids rendered hydrophilic by glow discharge at low pressures. Grids were washed with double distilled water and stained with 0.75% uranyl formate. Electron micrograph images of rhodopsin•rHDL particles were recorded with a Hitachi H-7000 TEM operated at 100 kV.

CHAPTER 4

CONCLUSIONS

Summary

The concept that GPCRs can associate as physical oligomeric complexes has been a controversial subject for many years. As data supporting this idea has emerged, the phenomenon of GPCR dimerization has become relatively well accepted. But along with this acceptance came questions as to the functional significance of GPCR dimerization. Many had postulated that since GPCRs do indeed dimerize, then the dimeric interaction must therefore be required for function, namely G protein activation. This evolved as a fundamental question regarding the mechanism of these important drug targets.

Prior to the development of the reconstituted HDL system, there was no definitive way to test this hypothesis in a rigorous, reductionist manner. By adapting the rHDL system for studying GPCRs, we were able to circumvent the inherent limitations of standard membrane protein biochemical techniques and isolate monomeric receptors in phospholipids bilayers. With the β_2AR, we showed that a monomeric receptor could efficiently couple to and activate a G protein [51]. We also demonstrated that the cooperativity observed with agonist binding to β_2AR, like many others members of the GPCR family, can be accounted for by direct G protein association, and not oligomerization – *i.e.* G proteins directly and allosterically modulate agonist binding to the receptor. Likewise, we relied on the unique organization of rhodopsin in specialized

tissues in the retina to show that monomeric rhodopsin is functionally identical to oligomeric rhodopsin *in vivo* [52].

Because we see little difference in function between monomeric and natively oligomeric receptors, we reason that dimerization plays little to no role in regards to G protein activation. In fact, this observation has also been recently confirmed, to a degree, by two separate labs, both studying rhodopsin. The Oprian lab, in collaboration with the Silgar lab, was able to incorporate one or two rhodopsins per HDL particle and observed that the HDL particles with two rhodopsins were approximately half as active as the monomer in terms of activating transducin [90]. However, the Sakmar lab, using a similar approach, observed that preparations containing two rhodopsins were actually comprised of a mixture of parallel and anti-parallel dimers (***Fig. 4-1***) [43]. It is assumed, but not yet demonstrated, that a similar distribution of parallel and anti-parallel dimers would be present in the Oprian/Sligar particles. Although the Sakmar lab also observed that transducin activation was half as efficient for two rhodopsins, they reasoned that the anti-parallel dimers were, however, non-functional. This assumption may be over-speculative based upon the presented data. An alternative interpretation and scenario could suggest that anti-parallel dimers are 90% as active as monomers and parallel dimers are 10% as active. The stochastic average would suggest that the dimers were half as active as monomers and lead to a dramatically different conclusion. The best way to avoid these confounding problems in interpreting the data is to isolate pure GPCR preparations of only parallel dimers. This is an extremely challenging task and is an approach that I have spent considerable time developing, but is unfortunately beyond of the scope of this thesis.

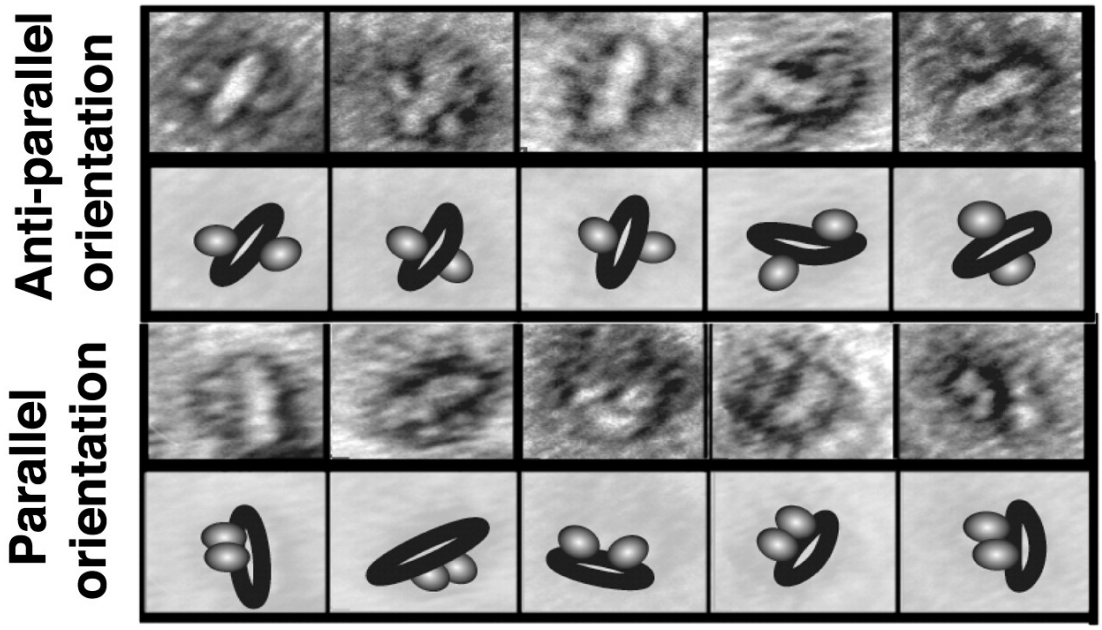

Figure 4-1. Visualization of rhodopsin in HDL using electron microscopy. Image adapted from Banerjee *et al.* [43] with permission. They used nanogold-labeled Fab fragments to label the rhodopsin in the HDL particles to elucidate their relative orientation. The Fab fragment is observed as an extra region of low density on the periphery of the HDL particle (white region surrounded by black ring). They observed an equal distribution of both parallel and anti-parallel orientations. Preparing samples of all parallel receptor dimers represents a challenging task but will be a necessary development for using the HDL system to study GPCR heterodimerization or arrestin signaling.

Is There a Functional Role for Dimerization?

Although we think that dimerization plays little to no role in G protein activation, it is still worth speculating as to a physiological/functional role of GPCR dimerization, since the evidence that GPCR dimers exist is still compelling. As mentioned earlier, clear targeting roles have been implicated for some GPCRs, such as the $GABA_B$ and α_{1D} receptors [29-32]. This may turn out to be a more common mechanism for other recalcitrant receptors, or for yet to be discovered orphan receptors. In a related vein, another likely possibility is that receptor oligomers exist solely on account of receptors

having a natural affinity for each other. This affinity could afford an extra quaternary language for dictating the organization of receptors as well as other proteins (i.e. effector proteins such as adenylyl cyclase or GIRK channels) into signalosome compartments to allow for more efficient signal transduction.

There are also several studies that have revealed interesting ligand binding data that suggest that dimerization may mediate receptor-receptor cross-talk, or cooperativity. One of the earliest of these studies attempted to show that co-expression of different opioid receptor heterodimers may affect their function [122]. A more recent study has implicated serotonin-glutamate receptor heterodimers in psychosis [123]. These are exciting studies that demonstrate interesting phenomena that may only exist with heterodimers, as a way to increase the natural receptor repertoire, and may not be manifested by homodimers. However, the interpretation of many of these results is confounded by cell-based systems and the lack of a rigorous demonstration of receptor dimerization. It would be useful to utilize the HDL system to address these questions.

Dimerization may also be important in regulating receptor desensitization. A dimeric cytosolic interface may have different affinities or reaction kinetics with the receptor kinase and arrestin desensitization machinery, when compared to a monomeric interface. Indeed, the crystal structure of arrestin reveals a double chalice-type shape [110-112] that is highly indicative of having a preferred interaction towards a receptor dimer (***Fig. 4-2***). Even more intriguing is the implication that receptor dimerization may play a role in regulating the G protein-independent signaling effects mediated by arrestin. The capacity of arrestin, like G proteins, to modulate agonist binding to β_2AR preparations reconstituted in phospholipid vesicles strongly supports this notion.

Likewise, these are all questions that application of the HDL reconstitution system is adeptly suited to answer.

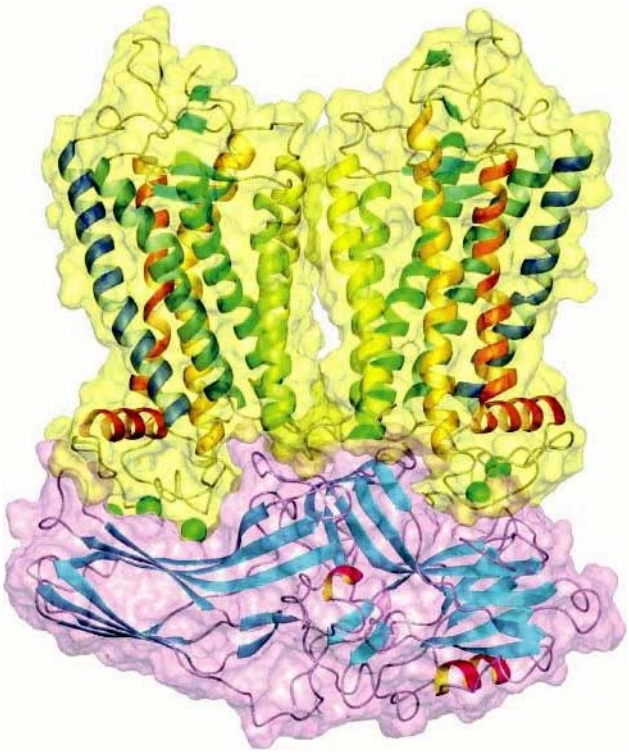

Figure 4-2. Molecular model of an arrestin-rhodopsin dimer complex. Arrestin (purple) has double-chalice-type structure that may have a preferential affinity for a rhodopsin dimer (yellow). Adapted from Park *et al.* [124] with permission.

Dimerization in Question

It should also be pointed out that the concept of GPCR dimerization has taken some hits in recent years. This is important to note because although our data do not rule out the existence of dimers, they are also completely compatible with the notion that dimers may not actually exist *in vivo*.

The strongest evidence to date against the prevailing GPCR dimer hypothesis comes from the Davis group[59]. In a rigorous study, they suggested that previous FRET and BRET experiments may have either been improperly executed or incorrectly

interpreted, and they actually concluded that the β_2AR does not dimerize using their methodology. This has generated considerable controversy in the field [125, 126] because RET experiments had heretofore been some of the best evidence that demonstrated that *bona fide* physical dimeric receptor interactions occurred in cells. The implications drawn here may influence the interpretation of published RET data concerning dozens of GPCRs.

The other pillar of evidence supporting GPCR dimerization, the AFM images showing paracrystalline arrays of rhodopsin dimers ROS discs [10], has also faced some criticism since its publication. Marc Chabre and others have claimed that the AFM data are the result of structural artifact resulting from sample preparation and that they defy a plethora of previous biophysical data that support the concept of rhodopsin as a monomeric and freely diffusing entity [33]. More importantly, this observation has yet to be repeated. In fact, using an ostensibly more native technique, the Palczewski lab imaged intact rod cells using cryoelectron tomography and did not observe any paracrystalline arrangement of rhodopsin [127].

It is clear that the field would benefit from more definitive proof or denial of the existence of GPCR dimers *in vivo*. New imaging or biophysical techniques are needed to observe the true native oligomeric state of GPCRs in primary tissue culture or in unperturbed tissues.

General applications of HDL technology

The technique of *in vitro* HDL reconstitution has been around for over 20 years, but has only been adapted to studying integral membrane biochemistry with in the last 5

years or so. Since then, the approach is gaining acceptance as a valid and superior method for studying membrane proteins. The Sligar lab first used the technology for studying P450 enzymes [68] and the bacteriorhodopsin ion channel [47], but other labs have since used HDL to study chemoreceptors [128], amphotericin B [129], and of course GPCRs [43, 51, 52, 90]. Over time, other labs will surely turn towards HDL for studying their protein of interest.

The absence of detergent and the mono-dispersed characteristics of HDL particles allow for the application of many biochemical and biophysical techniques that are not possible with other cell membrane-mimetic systems when detergent-based systems are not suitable. These include many types of assays that are taken for granted with soluble proteins, such as protein-protein interaction kinetics, novel ligand screening, proteomics, and of course standard enzymatic assays where detergents would have a deleterious effect.

As an example, we have taken fluorophore-labeled preparations of the β_2AR and studied their behavior in HDL particles. In collaboration with Dr. Brian Kobilka, we have now recapitulated the conformational changes observed with agonist binding to detergent preparations of monobromobimane-labeled β_2AR. More importantly we have recently observed a strong allosteric role of G proteins on agonist binding that is consistent with our observations using radioligand binding assays. The attributes of the HDL approach are perfectly suited to monitor the receptor conformations by fluorescence spectroscopy. In fact, we are now applying single molecule spectroscopy approaches using total internal reflection fluorescence (TIRF) microscopy to study receptor conformation.

HDL may also be an attractive platform for structural studies of membrane proteins. Since HDL itself has been described as a "molten" complex, X-ray crystallography may not be feasible unless the protein inserted into HDL's bilayer can be sufficiently stabilized by other protein-protein interactions within the crystal lattice. Cryo-electron microscopy, although lower resolution, may prove to be the most tractable approach. The natural mono-dispersion of HDL particles is well suited to the single particle reconstruction technique of building a three-dimensional structure from EM data. Indeed, our lab has initiated successful preliminary studies using this technique (***Fig. 4-3***). NMR may also prove to be a valuable method, and some groups have already initiated such studies [130, 131].

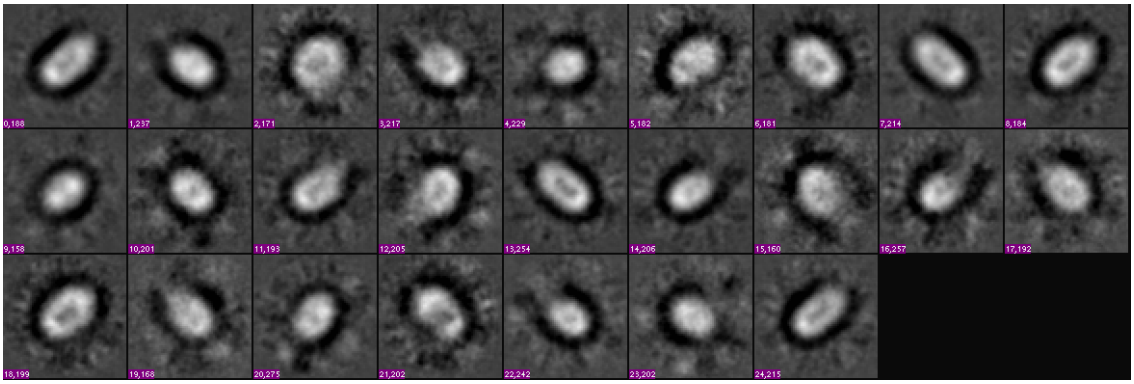

Figure 4-3. Cryo-EM class averages of HDL. In collaboration with Wah Chiu at the National Center for Macromolecular Imaging at Baylor College, we have started using the cryo-EM technique to gain structural information about HDL particles. Seen here are the class averages of several thousand HDL particles in vitrified ice. Each panel represents a group of HDL particles in a particular orientation. The main structural features are clearly seen: the apoAI belt (black ring) and the phospholipid bilayer (inner gray mass). With refinement of the technique, we hope to use this system as a platform for structural studies of membrane proteins.

An interesting feature of HDL is that it is amenable to extensive re-engineering since apoA-I can be expressed recombinantly. The Sligar lab has been able to duplicate internal apoAI segments to effectively increase the diameter of the HDL disc to 13 nm [132], and I have been able to increase this further to 16 nm (data not shown). These

advancements will undoubtedly aid the adoption of the HDL system to studying large proteins or multimeric protein complexes.

In summary, we have utilized this very powerful HDL approach to address an extremely controversial but fundamental aspect of GPCR signaling. We have successfully isolated monomeric GPCRs in a phospholipid bilayer and demonstrated efficient coupling to G proteins. The efficiency of this coupling is comparable with that observed in native membranes. We have also demonstrated that complex allosteric properties of agonist binding to the β_2AR, and perhaps other members of the Class A receptors are largely attributable to direct G protein allostery, and not receptor oligomerization, as previously postulated in the field. Together, these data support the notion that the monomeric GPCR, at least for the Class A family of receptors, is the minimal functional unit that couples to G proteins.

REFERENCES

1. Marinissen, M.J. and J.S. Gutkind, *G-protein-coupled receptors and signaling networks: emerging paradigms.* Trends Pharmacol Sci, 2001. **22**(7): p. 368-76.
2. Gilman, A.G., *G proteins: transducers of receptor-generated signals.* Annu Rev Biochem, 1987. **56**: p. 615-49.
3. Herrmann, R., et al., *Rhodopsin-transducin coupling: role of the Galpha C-terminus in nucleotide exchange catalysis.* Vision Res, 2006. **46**(27): p. 4582-93.
4. Kisselev, O.G. and M.A. Downs, *Rhodopsin-interacting surface of the transducin gamma subunit.* Biochemistry, 2006. **45**(31): p. 9386-92.
5. Neubig, R.R. and D.P. Siderovski, *Regulators of G-protein signalling as new central nervous system drug targets.* Nat Rev Drug Discov, 2002. **1**(3): p. 187-97.
6. Kwok-Keung Fung, B. and L. Stryer, *Photolyzed rhodopsin catalyzes the exchange of GTP for bound GDP in retinal rod outer segments.* Proc Natl Acad Sci U S A, 1980. **77**(5): p. 2500-4.
7. De Lean, A., J.M. Stadel, and R.J. Lefkowitz, *A ternary complex model explains the agonist-specific binding properties of the adenylate cyclase-coupled beta-adrenergic receptor.* J Biol Chem, 1980. **255**(15): p. 7108-17.
8. Wald, G., *Molecular basis of visual excitation.* Science, 1968. **162**(850): p. 230-9.
9. Palczewski, K., *G protein-coupled receptor rhodopsin.* Annu Rev Biochem, 2006. **75**: p. 743-67.
10. Fotiadis, D., et al., *Atomic-force microscopy: Rhodopsin dimers in native disc membranes.* Nature, 2003. **421**(6919): p. 127-8.
11. Lefkowitz, R.J. and S.K. Shenoy, *Transduction of receptor signals by beta-arrestins.* Science, 2005. **308**(5721): p. 512-7.
12. Violin, J.D. and R.J. Lefkowitz, *Beta-arrestin-biased ligands at seven-transmembrane receptors.* Trends Pharmacol Sci, 2007. **28**(8): p. 416-22.
13. Drake, M.T., et al., *beta-arrestin-biased agonism at the beta2-adrenergic receptor.* J Biol Chem, 2008. **283**(9): p. 5669-76.
14. Limbird, L.E., P.D. Meyts, and R.J. Lefkowitz, *Beta-adrenergic receptors: evidence for negative cooperativity.* Biochem Biophys Res Commun, 1975. **64**(4): p. 1160-8.
15. Seeman, P., et al., *The cloned dopamine D2 receptor reveals different densities for dopamine receptor antagonist ligands. Implications for human brain positron emission tomography.* Eur J Pharmacol, 1992. **227**(2): p. 139-46.
16. Fraser, C.M. and J.C. Venter, *The size of the mammalian lung beta 2-adrenergic receptor as determined by target size analysis and immunoaffinity chromatography.* Biochem Biophys Res Commun, 1982. **109**(1): p. 21-9.

17. Venter, J.C., et al., *The sequence of the human genome.* Science, 2001. **291**(5507): p. 1304-51.
18. Herberg, J.T., et al., *The hepatic glucagon receptor. Solubilization, characterization, and development of an affinity adsorption assay for the soluble receptor.* J Biol Chem, 1984. **259**(14): p. 9285-94.
19. Maggio, R., Z. Vogel, and J. Wess, *Coexpression studies with mutant muscarinic/adrenergic receptors provide evidence for intermolecular "cross-talk" between G-protein-linked receptors.* Proc Natl Acad Sci U S A, 1993. **90**(7): p. 3103-7.
20. Monnot, C., et al., *Polar residues in the transmembrane domains of the type 1 angiotensin II receptor are required for binding and coupling. Reconstitution of the binding site by co-expression of two deficient mutants.* J Biol Chem, 1996. **271**(3): p. 1507-13.
21. Pascal, G. and G. Milligan, *Functional complementation and the analysis of opioid receptor homodimerization.* Mol Pharmacol, 2005. **68**(3): p. 905-15.
22. Bouvier, M., *Oligomerization of G-protein-coupled transmitter receptors.* Nat Rev Neurosci, 2001. **2**(4): p. 274-86.
23. Hebert, T.E., et al., *A peptide derived from a beta2-adrenergic receptor transmembrane domain inhibits both receptor dimerization and activation.* J Biol Chem, 1996. **271**(27): p. 16384-92.
24. Devi, L.A., *Heterodimerization of G-protein-coupled receptors: pharmacology, signaling and trafficking.* Trends Pharmacol Sci, 2001. **22**(10): p. 532-7.
25. Lichtenberg, D., F.M. Goni, and H. Heerklotz, *Detergent-resistant membranes should not be identified with membrane rafts.* Trends Biochem Sci, 2005. **30**(8): p. 430-6.
26. Overton, M.C. and K.J. Blumer, *G-protein-coupled receptors function as oligomers in vivo.* Curr Biol, 2000. **10**(6): p. 341-4.
27. Angers, S., et al., *Detection of beta 2-adrenergic receptor dimerization in living cells using bioluminescence resonance energy transfer (BRET).* Proc Natl Acad Sci U S A, 2000. **97**(7): p. 3684-9.
28. Lakowicz, J.R., *Principles of Fluorescence Spectroscopy*. 3rd. ed. 1999: Springer. 725.
29. White, J.H., et al., *Heterodimerization is required for the formation of a functional GABA(B) receptor.* Nature., 1998. **396**(6712): p. 679-82.
30. Kaupmann, K., et al., *GABA(B)-receptor subtypes assemble into functional heteromeric complexes.* Nature., 1998. **396**(6712): p. 683-7.
31. Jones, K.A., et al., *GABA(B) receptors function as a heteromeric assembly of the subunits GABA(B)R1 and GABA(B)R2.* Nature., 1998. **396**(6712): p. 674-9.
32. Hague, C., et al., *Cell surface expression of alpha1D-adrenergic receptors is controlled by heterodimerization with alpha1B-adrenergic receptors.* J Biol Chem, 2004. **279**(15): p. 15541-9.
33. Chabre, M., R. Cone, and H. Saibil, *Biophysics: is rhodopsin dimeric in native retinal rods?* Nature, 2003. **426**(6962): p. 30-1; discussion 31.
34. Baneres, J.L. and J. Parello, *Structure-based analysis of GPCR function: evidence for a novel pentameric assembly between the dimeric leukotriene B4 receptor BLT1 and the G-protein.* J Mol Biol, 2003. **329**(4): p. 815-29.

35. Filipek, S., et al., *A concept for G protein activation by G protein-coupled receptor dimers: the transducin/rhodopsin interface.* Photochem Photobiol Sci, 2004. **3**(6): p. 628-38.
36. Christopoulos, A. and T. Kenakin, *G protein-coupled receptor allosterism and complexing.* Pharmacol Rev, 2002. **54**(2): p. 323-74.
37. Cha, K., P.J. Reeves, and H.G. Khorana, *Structure and function in rhodopsin: destabilization of rhodopsin by the binding of an antibody at the N-terminal segment provides support for involvement of the latter in an intradiscal tertiary structure.* Proc Natl Acad Sci U S A, 2000. **97**(7): p. 3016-21.
38. Ramon, E., et al., *Effect of dodecyl maltoside detergent on rhodopsin stability and function.* Vision Res, 2003. **43**(28): p. 3055-61.
39. Vogel, R., et al., *Deactivation of rhodopsin in the transition from the signaling state meta II to meta III involves a thermal isomerization of the retinal chromophore C[double bond]D.* Biochemistry, 2003. **42**(33): p. 9863-74.
40. Cerione, R.A. and E.M. Ross, *Reconstitution of receptors and G proteins in phospholipid vesicles.* Methods Enzymol, 1991. **195**: p. 329-42.
41. Degrip, W.J., J. Vanoostrum, and P.H. Bovee-Geurts, *Selective detergent-extraction from mixed detergent/lipid/protein micelles, using cyclodextrin inclusion compounds: a novel generic approach for the preparation of proteoliposomes.* Biochem J, 1998. **330 (Pt 2)**: p. 667-74.
42. Fung, B.K. and W.L. Hubbell, *Organization of rhodopsin in photoreceptor membranes. 1. Proteolysis of bovine rhodopsin in native membranes and the distribution of sulfhydryl groups in the fragments.* Biochemistry, 1978. **17**(21): p. 4396-402.
43. Banerjee, S., T. Huber, and T.P. Sakmar, *Rapid incorporation of functional rhodopsin into nanoscale apolipoprotein bound bilayer (NABB) particles.* J Mol Biol, 2008. **377**(4): p. 1067-81.
44. Mansoor, S.E., K. Palczewski, and D.L. Farrens, *Rhodopsin self-associates in asolectin liposomes.* Proc Natl Acad Sci U S A, 2006. **103**(9): p. 3060-5.
45. Bayburt, T.H., J.W. Carlson, and S.G. Sligar, *Reconstitution and imaging of a membrane protein in a nanometer-size phospholipid bilayer.* J Struct Biol, 1998. **123**(1): p. 37-44.
46. Baas, B.J., I.G. Denisov, and S.G. Sligar, *Homotropic cooperativity of monomeric cytochrome P450 3A4 in a nanoscale native bilayer environment.* Arch Biochem Biophys, 2004. **430**(2): p. 218-28.
47. Bayburt, T.H. and S.G. Sligar, *Self-assembly of single integral membrane proteins into soluble nanoscale phospholipid bilayers.* Protein Sci, 2003. **12**(11): p. 2476-81.
48. Lewis, G.F., *Determinants of plasma HDL concentrations and reverse cholesterol transport.* Curr Opin Cardiol, 2006. **21**(4): p. 345-52.
49. Matz, C.E. and A. Jonas, *Micellar complexes of human apolipoprotein A-I with phosphatidylcholines and cholesterol prepared from cholate-lipid dispersions.* J Biol Chem, 1982. **257**(8): p. 4535-40.
50. Jonas, A., *Reconstitution of high-density lipoproteins.* Methods Enzymol, 1986. **128**: p. 553-82.

51. Whorton, M.R., et al., *A monomeric G protein-coupled receptor isolated in a high-density lipoprotein particle efficiently activates its G protein.* Proc Natl Acad Sci U S A, 2007. **104**(18): p. 7682-7.
52. Whorton, M.R., et al., *Efficient coupling of transducin to monomeric rhodopsin in a phospholipid bilayer.* J Biol Chem, 2008. **283**(7): p. 4387-94.
53. Catterall, W.A., *Structure and function of voltage-gated ion channels.* Annu Rev Biochem, 1995. **64**: p. 493-531.
54. Clapham, D.E., L.W. Runnels, and C. Strubing, *The TRP ion channel family.* Nat Rev Neurosci, 2001. **2**(6): p. 387-96.
55. Dingledine, R., et al., *The glutamate receptor ion channels.* Pharmacol Rev, 1999. **51**(1): p. 7-61.
56. Schlessinger, J., *Cell signaling by receptor tyrosine kinases.* Cell., 2000. **103**(2): p. 211-25.
57. Chabre, M. and M. le Maire, *Monomeric G-protein-coupled receptor as a functional unit.* Biochemistry, 2005. **44**(27): p. 9395-403.
58. Fotiadis, D., et al., *Structure of the rhodopsin dimer: a working model for G-protein-coupled receptors.* Curr Opin Struct Biol, 2006. **16**(2): p. 252-9.
59. James, J.R., et al., *A rigorous experimental framework for detecting protein oligomerization using bioluminescence resonance energy transfer.* Nat Methods, 2006. **3**(12): p. 1001-6.
60. Hague, C., et al., *Cell surface expression of alpha1D-adrenergic receptors is controlled by heterodimerization with alpha1B-adrenergic receptors.* The Journal of biological chemistry., 2004. **279**(15): p. 15541-9.
61. Uberti, M.A., et al., *Heterodimerization with beta2-adrenergic receptors promotes surface expression and functional activity of alpha1D-adrenergic receptors.* The Journal of pharmacology and experimental therapeutics., 2005. **313**(1): p. 16-23.
62. Angers, S., et al., *Detection of beta 2-adrenergic receptor dimerization in living cells using bioluminescence resonance energy transfer (BRET).* Proceedings of the National Academy of Sciences of the United States of America., 2000. **97**(7): p. 3684-9.
63. Overton, M.C. and K.J. Blumer, *G-protein-coupled receptors function as oligomers in vivo.* Current biology : CB., 2000. **10**(6): p. 341-4.
64. Guo, W., L. Shi, and J.A. Javitch, *The fourth transmembrane segment forms the interface of the dopamine D2 receptor homodimer.* The Journal of biological chemistry., 2003. **278**(7): p. 4385-8.
65. Fotiadis, D., et al., *Atomic-force microscopy: Rhodopsin dimers in native disc membranes.* Nature., 2003. **421**(6919): p. 127-8.
66. El-Asmar, L., et al., *Evidence for negative binding cooperativity within CCR5-CCR2b heterodimers.* Mol Pharmacol, 2005. **67**(2): p. 460-9.
67. Baneres, J.L., et al., *Structure-based analysis of GPCR function: conformational adaptation of both agonist and receptor upon leukotriene B4 binding to recombinant BLT1.* J Mol Biol, 2003. **329**(4): p. 801-14.
68. Bayburt, T.H. and S.G. Sligar, *Single-molecule height measurements on microsomal cytochrome P450 in nanometer-scale phospholipid bilayer disks.* Proc Natl Acad Sci U S A, 2002. **99**(10): p. 6725-30.

69. Leitz, A.J., et al., *Functional reconstitution of Beta2-adrenergic receptors utilizing self-assembling Nanodisc technology.* Biotechniques, 2006. **40**(5): p. 601-2, 604, 606, passim.
70. Segrest, J.P., et al., *A detailed molecular belt model for apolipoprotein A-I in discoidal high density lipoprotein.* J Biol Chem, 1999. **274**(45): p. 31755-8.
71. Palczewski, K., et al., *Crystal structure of rhodopsin: A G protein-coupled receptor.* Science, 2000. **289**(5480): p. 739-45.
72. Neubig, R.R., R.D. Gantzos, and W.J. Thomsen, *Mechanism of agonist and antagonist binding to alpha 2 adrenergic receptors: evidence for a precoupled receptor-guanine nucleotide protein complex.* Biochemistry, 1988. **27**(7): p. 2374-84.
73. Mukhopadhyay, S. and E.M. Ross, *Rapid GTP binding and hydrolysis by G(q) promoted by receptor and GTPase-activating proteins.* Proc Natl Acad Sci U S A, 1999. **96**(17): p. 9539-44.
74. Biddlecome, G.H., G. Berstein, and E.M. Ross, *Regulation of phospholipase C-beta1 by Gq and m1 muscarinic cholinergic receptor. Steady-state balance of receptor-mediated activation and GTPase-activating protein-promoted deactivation.* J Biol Chem, 1996. **271**(14): p. 7999-8007.
75. Seifert, R., et al., *Different effects of Gsalpha splice variants on beta2-adrenoreceptor-mediated signaling. The beta2-adrenoreceptor coupled to the long splice variant of Gsalpha has properties of a constitutively active receptor.PG - 5109-16.* J Biol Chem, 1998. **273**(9).
76. Kent, R.S., A. De Lean, and R.J. Lefkowitz, *A quantitative analysis of beta-adrenergic receptor interactions: resolution of high and low affinity states of the receptor by computer modeling of ligand binding data.* Mol Pharmacol, 1980. **17**(1): p. 14-23.
77. Guo, W., L. Shi, and J.A. Javitch, *The fourth transmembrane segment forms the interface of the dopamine D2 receptor homodimer.* J Biol Chem, 2003. **278**(7): p. 4385-8.
78. Galvez, T., et al., *Allosteric interactions between GB1 and GB2 subunits are required for optimal GABA(B) receptor function.* Embo J, 2001. **20**(9): p. 2152-9.
79. Lavoie, C., et al., *Beta 1/beta 2-adrenergic receptor heterodimerization regulates beta 2-adrenergic receptor internalization and ERK signaling efficacy.* J Biol Chem, 2002. **277**(38): p. 35402-10.
80. Goudet, C., et al., *Asymmetric functioning of dimeric metabotropic glutamate receptors disclosed by positive allosteric modulators.* J Biol Chem, 2005. **280**(26): p. 24380-5.
81. Kobilka, B.K., *Amino and carboxyl terminal modifications to facilitate the production and purification of a G protein-coupled receptor.* Anal Biochem, 1995. **231**(1): p. 269-71.
82. Gan, K.N., et al., *Purification of human serum paraoxonase/arylesterase. Evidence for one esterase catalyzing both activities.* Drug Metab Dispos, 1991. **19**(1): p. 100-6.
83. Huang, B., T.D. Perroud, and R.N. Zare, *Photon counting histogram: one-photon excitation.* Chemphyschem, 2004. **5**(10): p. 1523-31.

84. Kozasa, T. and A.G. Gilman, *Purification of recombinant G proteins from Sf9 cells by hexahistidine tagging of associated subunits. Characterization of alpha 12 and inhibition of adenylyl cyclase by alpha z.* J Biol Chem, 1995. **270**(4): p. 1734-41.
85. Asano, T., et al., *Reconstitution of catecholamine-stimulated binding of guanosine 5'-O-(3-thiotriphosphate) to the stimulatory GTP-binding protein of adenylate cyclase.* Biochemistry, 1984. **23**(23): p. 5460-7.
86. Yao, X., et al., *Coupling ligand structure to specific conformational switches in the beta2-adrenoceptor.* Nat Chem Biol, 2006. **2**(8): p. 417-22.
87. Venter, J.C., et al., *The sequence of the human genome.* Science, 2001. **291**(5507): p. 1304-51.
88. Angers, S., A. Salahpour, and M. Bouvier, *Dimerization: an emerging concept for G protein-coupled receptor ontogeny and function.* Annu Rev Pharmacol Toxicol, 2002. **42**: p. 409-35.
89. Leitz, A.J., et al., *Functional reconstitution of Beta2-adrenergic receptors utilizing self-assembling Nanodisc technology.* Biotechniques, 2006. **40**(5): p. 601-606.
90. Bayburt, T.H., et al., *Transducin activation by nanoscale lipid bilayers containing one and two rhodopsins.* J Biol Chem, 2007. **282**(20): p. 14875-81.
91. Ridge, K.D. and K. Palczewski, *Visual rhodopsin sees the light: structure and mechanism of G protein signaling.* J Biol Chem, 2007. **282**(13): p. 9297-301.
92. O'Brien, D.F., L.F. Costa, and R.A. Ott, *Photochemical functionality of rhodopsin-phospholipid recombinant membranes.* Biochemistry, 1977. **16**(7): p. 1295-303.
93. Jonas, A., et al., *Apolipoprotein A-I structure and lipid properties in homogeneous, reconstituted spherical and discoidal high density lipoproteins.* J Biol Chem, 1990. **265**(36): p. 22123-9.
94. Segrest, J.P., et al., *Structure and function of apolipoprotein A-I and high-density lipoprotein.* Curr Opin Lipidol, 2000. **11**(2): p. 105-15.
95. Forte, T.M. and R.W. Nordhausen, *Electron microscopy of negatively stained lipoproteins.* Methods Enzymol, 1986. **128**: p. 442-57.
96. Jones, A.L. and J.M. Price, *Some methods of electron microscopic visualization of lipoproteins in plasma and chyle.* J Histochem Cytochem, 1968. **16**(5): p. 366-70.
97. Jones, K.A., et al., *GABA(B) receptors function as a heteromeric assembly of the subunits GABA(B)R1 and GABA(B)R2.* Nature, 1998. **396**(6712): p. 674-9.
98. Baldwin, P.A. and W.L. Hubbell, *Effects of lipid environment on the light-induced conformational changes of rhodopsin. 2. Roles of lipid chain length, unsaturation, and phase state.* Biochemistry, 1985. **24**(11): p. 2633-9.
99. Farrens, D.L. and H.G. Khorana, *Structure and function in rhodopsin. Measurement of the rate of metarhodopsin II decay by fluorescence spectroscopy.* J Biol Chem, 1995. **270**(10): p. 5073-6.
100. Jastrzebska, B., et al., *Functional and structural characterization of rhodopsin oligomers.* J Biol Chem, 2006. **281**(17): p. 11917-22.
101. Baehr, W., et al., *Characterization of bovine rod outer segment G-protein.* J Biol Chem, 1982. **257**(11): p. 6452-60.

102. Fahmy, K. and T.P. Sakmar, *Light-dependent transducin activation by an ultraviolet-absorbing rhodopsin mutant.* Biochemistry, 1993. **32**(35): p. 9165-71.
103. Jastrzebska, B., et al., *Functional characterization of rhodopsin monomers and dimers in detergents.* J Biol Chem, 2004. **279**(52): p. 54663-75.
104. Prinster, S.C., C. Hague, and R.A. Hall, *Heterodimerization of g protein-coupled receptors: specificity and functional significance.* Pharmacol Rev, 2005. **57**(3): p. 289-98.
105. White, J.H., et al., *Heterodimerization is required for the formation of a functional GABA(B) receptor.* Nature, 1998. **396**(6712): p. 679-82.
106. Bulenger, S., S. Marullo, and M. Bouvier, *Emerging role of homo- and heterodimerization in G-protein-coupled receptor biosynthesis and maturation.* Trends Pharmacol Sci, 2005. **26**(3): p. 131-7.
107. Fotiadis, D., et al., *The G protein-coupled receptor rhodopsin in the native membrane.* FEBS Lett, 2004. **564**(3): p. 281-8.
108. Baylor, D.A., T.D. Lamb, and K.W. Yau, *Responses of retinal rods to single photons.* Journal of Physiology, 1979. **288**: p. 613-634.
109. Duthey, B., et al., *A single subunit (GB2) is required for G-protein activation by the heterodimeric GABA(B) receptor.* J Biol Chem, 2002. **277**(5): p. 3236-41.
110. Hirsch, J.A., et al., *The 2.8 A crystal structure of visual arrestin: a model for arrestin's regulation.* Cell, 1999. **97**(2): p. 257-69.
111. Skegro, D., et al., *N-terminal and C-terminal Domains of Arrestin Both Contribute in Binding to Rhodopsin(dagger).* Photochem Photobiol, 2006.
112. Modzelewska, A., et al., *Arrestin interaction with rhodopsin: conceptual models.* Cell Biochem Biophys, 2006. **46**(1): p. 1-15.
113. Lambright, D.G., et al., *Structural determinants for activation of the alpha-subunit of a heterotrimeric G protein.* Nature, 1994. **369**(6482): p. 621-8.
114. Lefkowitz, R.J., K. Rajagopal, and E.J. Whalen, *New roles for beta-arrestins in cell signaling: not just for seven-transmembrane receptors.* Mol Cell, 2006. **24**(5): p. 643-52.
115. Okada, T., et al., *Methods and Results in X-Ray Crystallography of Bovine Rhodopsin*, in *G Protein-Coupled Receptors: Structure, Function, and Ligand Screening*, T. Haga, Editor. 2005, CRC Press LLC: Boca Raton, FL. p. 245-261.
116. Wald, G. and P.K. Brown, *The molar extinction of rhodopsin.* J Gen Physiol, 1953. **37**(2): p. 189-200.
117. Heck, M., et al., *Signaling states of rhodopsin. Formation of the storage form, metarhodopsin III, from active metarhodopsin II.* J Biol Chem, 2003. **278**(5): p. 3162-9.
118. De Grip, W.J., *Purification of bovine rhodopsin over concanavalin A--sepharose.* Methods Enzymol, 1982. **81**: p. 197-207.
119. Oprian, D.D., et al., *Expression of a synthetic bovine rhodopsin gene in monkey kidney cells.* Proc Natl Acad Sci U S A, 1987. **84**(24): p. 8874-8.
120. Pownall, H.J. and J.B. Massey, *Spectroscopic studies of lipoproteins.* Methods Enzymol, 1986. **128**: p. 515-8.
121. Fahmy, K. and T.P. Sakmar, *Regulation of the rhodopsin-transducin interaction by a highly conserved carboxylic acid group.* Biochemistry, 1993. **32**(28): p. 7229-36.

122. Jordan, B.A. and L.A. Devi, *G-protein-coupled receptor heterodimerization modulates receptor function.* Nature, 1999. **399**(6737): p. 697-700.
123. Gonzalez-Maeso, J., et al., *Identification of a serotonin/glutamate receptor complex implicated in psychosis.* Nature, 2008. **452**(7183): p. 93-7.
124. Park, P.S., et al., *Oligomerization of G protein-coupled receptors: past, present, and future.* Biochemistry, 2004. **43**(50): p. 15643-56.
125. Bouvier, M., et al., *BRET analysis of GPCR oligomerization: newer does not mean better.* Nat Methods, 2007. **4**(1): p. 3-4; author reply 4.
126. Salahpour, A. and B. Masri, *Experimental challenge to a 'rigorous' BRET analysis of GPCR oligomerization.* Nat Methods, 2007. **4**(8): p. 599-600; author reply 601.
127. Nickell, S., et al., *Three-dimensional architecture of murine rod outer segments determined by cryoelectron tomography.* J Cell Biol, 2007. **177**(5): p. 917-25.
128. Boldog, T., et al., *Nanodiscs separate chemoreceptor oligomeric states and reveal their signaling properties.* Proc Natl Acad Sci U S A, 2006. **103**(31): p. 11509-14.
129. Nelson, K.G., et al., *Nanodisk-associated amphotericin B clears Leishmania major cutaneous infection in susceptible BALB/c mice.* Antimicrob Agents Chemother, 2006. **50**(4): p. 1238-44.
130. Kijac, A.Z., et al., *Magic-angle spinning solid-state NMR spectroscopy of nanodisc-embedded human CYP3A4.* Biochemistry, 2007. **46**(48): p. 13696-703.
131. Li, Y., et al., *Structural analysis of nanoscale self-assembled discoidal lipid bilayers by solid-state NMR spectroscopy.* Biophys J, 2006. **91**(10): p. 3819-28.
132. Denisov, I.G., et al., *Directed self-assembly of monodisperse phospholipid bilayer Nanodiscs with controlled size.* J Am Chem Soc, 2004. **126**(11): p. 3477-87.